

On the Concentration of Water in Arc Basalts: case study in Izu Oshima, Miyakejima, Fuji and some perspectives

TAKAHASHI, Eiichi^{1*}, HAMADA, Morihisa¹, USHIODA, Masashi¹, ASANO, Kenta¹

¹Magma Factory, Earth & Planetary Sciences, Tokyo Institute of Technology

Genesis, transportation mechanism and distribution of water in subduction system is very important to understand various geological phenomena in subduction zones. Origin of subduction zone magma is thought to be deeply connected with dehydration of subducting slabs. Because water degassed from magma prior to or during volcanic eruption, concentration of water in arc magma is not well constrained. In this study, we show evidences that basalt magma in volcanic front generally contains several weight percent of water. This is in contrast with previous view on lateral variation of water in Japanese Quaternary volcanoes (Sakuyama, 1979; Aoki et al, 1981). It also contradicts with estimated geographical variation of fluid components in Japanese Quaternary volcanoes by Nakamura et al.(2008) and Nakamura & Iwamori (2010).

Based on high-pressure melting experiments on primitive basalt of Izu-Oshima volcano, Hamada & Fujii (2007) concluded that presence of 3 to 6 wt% of water is necessary in order to explain very calcic (~An90) plagioclase phenocryst. Phase relation of primitive basalt from Ofunato stage of Miyakejima volcano has been studied experimentally (Ushioda et al, 2011) and it is found that about 3 wt% of water is necessary in order to explain its phenocryst assemblage (ol + pl) and the calcic plagioclase composition (An90-94). Moreover, Hamada et al. (2011) has established a new method to estimate pre-degassing water content of magma using hydrogen concentration in plagioclase phenocryst. Using this new technique, water content in main magma chamber of Izu-Oshima volcano prior to 1986 eruption was estimated to be ~5 wt%.

Presence of large amount of water in basalt magma is also supported from explosive volcanic eruption style of Fuji volcano (e.g. Hoei sub-plinian eruption of 1707). According to Machida (1977), amount of volcanic ash (tephra) from Fuji volcano may be equal or greater than its volcanic edifice. This indicates that the explosive eruption style of Fuji volcano continued through time and therefore high water content in its basalt magma is a continuous feature.

Basalt magma is less abundant in the volcanoes on Honshu Arc due to the extensive fractionation, magma mixing and crustal melting. Precise estimate of water content in their primitive basalt magma is therefore difficult. However, presence of very high modal amount of plagioclase phenocryst in basalt and basaltic andesite (usually 30~40 vol%), is a good indication of the presence of large amount of water in these mafic magmas. This is because, degassing of hydrous basalt at shallow magma chamber invariably accompanies crystallization of large amount of plagioclase (e.g., Hamada & Fujii, 2008).

We therefore propose that basalt magma in volcanic front of Izu Mariana Arc (e.g., Fuji, Izu-Oshima, Miyakejima) and those of North Honshu Arc are all wet, may be typically containing 5 wt% of water or even higher. This view strongly contradicts with previous works; 1) lateral variation of water content similar to potassium (Sakuyama, 1979; Aoki et al, 1981); 2) nearly anhydrous magma genesis model by Tatsumi et al.(1983) at the volcanic front, and 3) recent estimation of fluid component in magma based on systematics in Nd and Pb isotopes (e.g. Nakamura & Iwamori, 2010). Our model, however, is not inconsistent with a model proposed by Kimura et al.(2010). We will discuss origin of the discrepancy between our model and previous works. We will also emphasize the importance of the large water flux released by hydrous basalt magma at the volcanic front in considering circulation of water in subduction zone.

Keywords: magma, water content, basalt, island arc, volcano

Volatile behaviors in an immature subduction zone inferred from boninitic melt inclusions

SHIMIZU, Kenji^{1*}, SHIMIZU, Nobumichi²

¹JAMSTEC, ²WHOI

Recent study suggests that boninites formed at the immature stage of subduction zone, whereas related arc tholeiites erupted 0-7 Ma after boninite formations (Ishizuka et al., 2011, EPSL, v306, p229-240). In order to constrain volatile behaviors of an immature subduction zone, we have analyzed major, volatile contents and sulfur isotopic ratios ($^{34}\text{S}/^{32}\text{S}$) of melt inclusions in Cr-spinel from fore-arc volcanic rocks in Bonin Islands and in Guam. All Cr-spinels are collected at volcanic sand beaches and purified for this study. Boninitic melt inclusions occur in Muko-jima, Chichi-jima and tholeiitic melt inclusions occur in Mukoo-jima and Guam. Cr-spinels in boninite are high in Cr# (mostly 80-90) and low in TiO₂ (< 0.1wt%), indicating highly depleted source. Whereas Cr-spinels in tholeiite vary in Cr# (45-80) and in TiO₂ (0.1-1 wt%). Compositions of melt inclusions fully cover compositional range of whole-rock. Some melt inclusions of boninites have MgO higher than 20 wt%, showing that they are very primitive magmas. H₂O and CO₂ contents of melt inclusions of Muko-jima boninite are high (up to 4 wt%) and low (< 50 ppm), respectively whereas those of Mukoo-jima tholeiite are lower (H₂O mostly ~1 wt%) and higher (CO₂ up to ~1000ppm). Except H₂O, volatiles of boninitic melt inclusions (F <20ppm; Cl <500ppm; S ~100ppm) are considerably lower than those in tholeiites (F up to 400ppm; Cl up to 3000ppm; S up to 3000ppm). High S content of tholeiitic melt inclusions may indicate high oxygen fugacity of the magmas. Sulfur isotope data of melt inclusions from boninites show the lightest value that reported from igneous rocks ($d^{34}\text{S}_{VCDT} = -5$ to -10), whereas those of tholeiites ($d^{34}\text{S}_{VCDT} = +2$ to $+5$) are comparable to reported arc tholeiite data. S source of tholeiite should be mixture of seawater-derived hydrothermal sulfites and mantle sulfide. Whereas S source of boninite can be seawater derived pyrite which precipitated in mantle, inorganically, because of reduced condition caused by water-mantle reaction. As source of boninite is hydrated hertzbergite, sulfur in the source before the hydration may be negligible. Therefore, all sulfur of boninite may be secondary origin. Assuming open system isotope fractionation, $d^{34}\text{S}_{VCDT}$ difference between seawater sulfate (20 permil) and pyrite (-5 to -10 permil) can be explained by pyrite precipitation at ~200°C, which is consistent temperature of serpentinization at subduction zone. Boninite may be formed by melting of this serpentinite at an immature stage. Further contaminations by fluid led higher oxygen fugacity at mantle wedge, forming arc tholeiites.

Keywords: boninite, arc tholeiite, sulfur isotope, volatiles, melt inclusion

The redox states of volcanic glasses from Bonin islands, Japan, estimated by Fe-K edge micro XANES study

ISHIBASHI, Hidemi^{1*}, ODAKE, Shoko², KANAYAMA, Kyoko³, HAMADA, Morihisa⁴, KAGI, Hiroyuki⁵

¹ERI, Univ. Tokyo, ²HIGP, Univ. Hawaii, ³Earth Sci., Kanazawa Univ., ⁴Department of Earth and Planetary Sciences, Tokyo Institute of Technology, ⁵Graduate School of Science, Univ. Tokyo

The redox state of arc mantle is an important issue to understand processes of material cycle and generation of magma within mantle wedge. Previous studies on mantle xenoliths indicated that arc mantle is more oxidized relative to those of other tectonic settings and proposed that the oxidized nature is attributed to an influence of subduction-related fluid. However, it is unobvious that partially melted region within mantle wedge where arc magma is generated is actually oxidized because mantle xenoliths are fragments of cool, rigid, re-equilibrated lithospheric mantle. In addition, the role of subduction-related fluid on oxidization of arc mantle is still unclear.

Arc magmas might be a unique material having information about the redox state of their source mantle region. Among various arc magmas, we thought that boninite is the most suitable to examine both the redox state of arc mantle and the effect of subduction-related fluid on arc mantle. This is because boninite is undifferentiated rock quenched in seawater. They are expected to preserve information on redox state of sub-arc mantle. In addition, they were considered to be generated by partial melting of hydrous mantle which was highly influenced by subduction-related fluid. Therefore, the redox state of boninite is expected to give clue to above issues.

It is well known that valence state of Fe in silicate glass is a sensitive indicator of its oxygen fugacity (fO_2). Recent advance in Fe-K edge micro-XANES (X-ray Absorption Near Edge Structure) study enables us to determine valence state of Fe in silicate glass with several microns order of special resolution. In this study, we investigated fO_2 of quenched silicate glasses included in pillow lavas and hyaloclastites of boninite from Chichijima, Otojima, and Mukojima, Bonin islands, Japan. We also analyzed quenched basaltic glasses from Anejima and Hahajima for comparison. In addition, quenched glasses of AIST standard rock samples (JA-1a, JA-2, and JB-2) synthesized at fO_2 near quartz-magnetite-fayalite (QMF) and Ni-NiO (NNO) buffers were analyzed to assess the reliability of this analytical method. We performed the measurements using Beam Line 4A in Photon Factory, KEK, which enables us micro analysis of XANES. The obtained spectra were analyzed using the method of Cottrell et al. (2009) to determine mole ratios of ferric to total iron, Fe^{3+}/Fe . Oxygen fugacity of silicate glass was calculated from the Fe^{3+}/Fe ratio using the method of Kress and Carmichael (1991). Reliability of our analyses is confirmed because controlled fO_2 during synthesizing standard glasses is reproduced within standard deviation of 0.4 by the models of Cottrell et al. (2009) and Kress and Carmichael (1991).

The measured Fe^{3+}/Fe ratios of quenched glasses are 0.17-0.24 for boninites from Chichijima, Otojima, and Mukojima. Basaltic glasses from Anejima and Hahajima are 0.20-0.22, which is identical to those of boninites. These values are larger than the average Fe^{3+}/Fe value of MORB (ca.0.16). We estimated fO_2 of the measured glasses is near NNO buffer based on obtained Fe^{3+}/Fe ratios. Because the effects of crystallization of silicate minerals and dehydration during ascent on fO_2 of silicate melt are thought to be small, the estimated fO_2 of the glasses may inherit their genetic conditions. Our results suggest that (1) slab-derived fluid related to boninite genesis did not significantly affect the redox state of source mantle region and (2) the redox state of arc mantle was oxidized even at an initial stage of arc evolution. This is inconsistent with the results of Lee et al. (2005, 2010).

Keywords: XANES, Oxygen fugacity, arc mantle, volcanic glass, boninite, Bonin islands

In-situ determination of Pb partition between aqueous fluids and haplogranite melts under HTHP conditions

KAWAMOTO, Tatsuhiko^{1*}, MIBE, Kenji², Helene Bureau³, Solenn Reguer⁴, Cristian Mocuta⁴, Stefan Kubsky⁵, Dominique Thiaudiere⁴, ONO, Shigeaki⁶, KOGISO, Tetsu⁷

¹Inst. Geothermal Sci., Kyoto Univ., ²ERI, Univ. Tokyo, ³IMPMC, Universite Paris VI et VII, ⁴DiffAbs beamline, Synchrotron SOLEIL, ⁵Surface Laboratory, Synchrotron SOLEIL, ⁶IFREE, JAMSTEC, ⁷Grad School Human & Environ. Kyoto Univ.

Using a micro-focused synchrotron x ray at Synchrotron SOLEIL (France), in-situ x-ray fluorescence (XRF) spectra of Pb, Rb, and Sr are obtained from aqueous fluids and haplogranite/jadeite melt at 0.3-1.3 GPa and 730-830C. Partition coefficients between aqueous fluids and melts are obtained for Pb, Sr and Rb ($D^{fluid/melt}_{Pb}$, $D^{fluid/melt}_{Rb}$, $D^{fluid/melt}_{Sr}$) with and without Cl. As pressure increases, $D^{fluid/melt}_{Pb}$, $D^{fluid/melt}_{Rb}$, and $D^{fluid/melt}_{Sr}$ increase. As salinity increases, $D^{fluid/melt}_{Pb}$, $D^{fluid/melt}_{Rb}$, and $D^{fluid/melt}_{Sr}$ increase. $D^{fluid/melt}_{Pb}$ are larger than unity in 5 M (Na, K)Cl bearing solution-haplogranite melt system. $D^{fluid/melt}_{Rb}$ are larger than unity in 2.5 M NaCl bearing solution-jadeite melt system. Under the identical conditions, $D^{fluid/melt}_{Sr}$ are smaller than 0.6 and 0.1, respectively. The present study confirms that saline fluids can transfer large ion lithophile elements such as Pb, Rb, and Sr from subducting oceanic lithosphere to the mantle wedge, whereas Cl-free aqueous fluids cannot.

Keywords: magma, aqueous fluid, elemental partition, high temperature and high pressure, synchrotron X-ray fluorescence, lead

Development of a database of the electrical conductivity of H₂O-NaCl fluids: A molecular dynamics study

SAKUMA, Hiroshi^{1*}, ICHIKI, Masahiro², FUJI-TA, Kiyoshi³, KAWAMURA, Katsuyuki⁴

¹Tokyo Institute of Technology, ²Tohoku University, ³Osaka University, ⁴Okayama University

Introduction: Fluids in the earth's crust would have large effects on the occurrence of earthquake and volcanic eruptions. To delineate distribution of the fluids in the earth's crust is requisite to understand the effects of the fluids on the earthquake and volcanic activities. The distribution of the fluids has been expected to be revealed by electromagnetic observation, e.g. magnetotellurics. Electrical conductivity distribution in the crust is considered to roughly correspond to the fluids distribution because of the high electrical conductivity of fluids relative to solids. To develop a plausible model of the fluids distribution to explain the electromagnetic observations, we have to construct a database of the electrical conductivities of fluids over the wide range of pressure (P), temperature (T), and electrolyte concentrations (c). The experimental approaches to measure the electrical conductivities of aqueous NaCl solution have been difficult at high P , T and c conditions and we can get only the data at $P < 4000$ bars, $T < 1100$ K and $c < 0.1$ m (mol/kg) [1]. Classical molecular dynamics (MD) simulations are useful to obtain the physical properties of fluids at high P , T and c conditions and to understand the underlying atomic-scale mechanism of the electrical conductivities. The phases of water and aqueous NaCl solutions at the P - T conditions of the Earth's crust are in liquid and supercritical states. The aims of this study are to make a reliable water model to simulate water in liquid and supercritical phases and to construct a database of electrical conductivity of aqueous NaCl solution at high temperature and pressure conditions.

Computational Methods: We have developed a flexible and polarizable water model based on our previous flexible model [2]. In our new model, the point charges are located on the hydrogen atoms and on the lone pairs of the oxygen atom. The point charges are fluctuated during the MD simulations. The MD simulations were performed using the code MXDORTO with some modifications.

Results and Discussion: Electrical conductivity of aqueous NaCl solution should depend on the density, viscosity, dielectric constant, and salt concentration (mol/kg) [1]. The density and salt concentration are the parameters of the number of ions per unit volume. In the atomic-scale view, the decrease of the viscosity corresponds to the increase of the ionic mobility. Since the viscosity sharply decreases with the increase of the temperature and shows no large dependence on P and T at $T > 600$ K, the density, salt concentration and dielectric constant are the most important parameters at $T > 600$ K. To construct a reliable water model for the supercritical phases, we should check the reproducibility of the physical properties compared with experimental results. Here we compared the structure, density, dielectric constants, and electrical conductivity of aqueous NaCl solutions in supercritical phases with some experiments. The radial distribution functions between atoms in the solution were good agreement with the experiments at 673 K and 3400 bar. The densities of 0.1 m NaCl solution and dielectric constants of water at $T = 573 \sim 973$ K and $P = 2000 \sim 5000$ bar were reasonable compared with the experiments. In this study, we explain the underlying mechanism of the change of the electrical conductivity of aqueous NaCl solution in the supercritical phase from atomistic view and try to construct the useful equations for the electrical conductivity of aqueous NaCl solution in the supercritical phase.

[1] Quist, A.S. and Marshall, W.L. (1968) JPC 72 684-703. [2] Kumagai, N., Kawamura, K. and Yokokawa, T. (1994) Mol. Simul. 12 177-186.

Keywords: dielectric constant, ion association, polarizable model, MD

Spatial distribution of slab-related fluid in Japan - Relation to inland earthquakes -

KAZAHAYA, Kohei^{1*}, HASEGAWA, Akira², TAKAHASHI, Masaaki¹, OYAMA, Yoichi³, TAKAHASHI, Hiroshi¹, IWAMORI, Hikaru⁴, MATSUZAWA, Toru², Tsukasa Kirita¹

¹Geological Survey of Japan, AIST, ²Research Center for Prediction of Earthquakes and Volcanic Eruptions, Tohoku Univ., ³Graduate School of Life and Environmental Science, University of Tsukuba, ⁴Department of Earth and Planetary Sciences, Tokyo Institute of Technology

Recently, possibility that fluids are involved in earthquakes has been pointed out. Activity of the deep low frequency (DLF) earthquakes and the shallow inland microquakes in Japan have been precisely monitored by the Hi-net for the last decade. The DLF earthquakes are well-determined for hypocenter having feature of very deep (20-40km depth) and thought to be related with hydrothermal fluids. In this study, we show the spatial distribution of crustal fluid and discuss the role of fluids in the occurrences of the DLF earthquake and the inland microquake.

Saline waters found close to the hypocenter of the DLF events show characteristic isotopic composition and chemistry; 1) similar to magmatic water or Arima-type thermal water indicated by isotopic composition of water, 2) NaCl-CO₂-type, and 3) high Li/Cl ratio (>0.001 in wt. ratio). The flow rate of these saline waters were hydrologically investigated at 6 places in Kinki district to be 8.5 kgH₂O/sec in total. Calculated dehydration rate of subducting slabs given from literatures ranged from 4 to 36 kgH₂O/sec for the arc length of 100km (SW Japan), which corresponds to our observational results, indicating they are of slab dehydration origin. The fluid involved in DLF events is likely either a magmatic fluid released during solidification of a magma at lower crust or a slab fluid directly supplied by slab dehydration.

The spatial distribution of slab-related fluids also agree well with that of shallow microquake occurrences (depth < 20km) or areas showing shallower D90 as well as that of DLF events. Upwelling of slab-related fluids seems to be one of the cause of shallow microquake activities. Fluids needs a path for upwelling such as a fissure existing at faults, and then the upwelling fluids will reduce the friction of fault planes. Furthermore, the recent large inland earthquakes ($M > 7$) occurred close to the area of DLF events where the slab-related fluid exists. And some areas (a part of Chugoku district and the Abukuma granitic province), where no slab-related fluids are found, has relatively less earthquake activity. In conclusion, the NaCl-CO₂-type slab-related fluid widely exists but is localized in Japan, and play a role on inland earthquake activity.

Keywords: crustal fluid, slab-related, inland earthquake, deep low frequency event

Groundwater database and its analysis utilizing the hot spring analysis table

SUGIMOTO, Masaaki^{1*}, TANAKA, Hidemi¹

¹Department of Earth and Planetary Science, Graduate school of Science, The University of Tokyo

It is known that the role of water in the material circulation in subduction zones is important. Since 2009, Tanaka laboratory, has been collecting its own the table hot spring analysis in cooperation with each prefectural government, the health center. These tables are based on Paragraph 1 of Article 18 of the Act in hot spring law. Because, results of the analysis, public secondary raw data is difficult of personal property. Currently, the database of the Tanaka laboratory in Japan but some areas are missed, the data is already entered into the GIS 5,998 points.

In addition to the introduction of the above database, to announce the results of the analysis. It was of particular interest this time is the ratio Br / Cl and Li / Cl . Kaga and Toyama Plain are adjacent plain. But, Na-Cl type hot springs wick exist at coastal area, that characteristic of Li/Cl and Br/Cl ratio are different. Also examine other areas, you can find similar characteristics of Br/Cl and Li/Cl to the group of Toyama Plain's Na-Cl type hot springs, that overlap with the hot springs considered affected by Arima-type deep brine.

Keywords: Hot springs, Groundwater database, GIS, Arima-type deep brine, Br/Cl , Li/Cl

Fluid inclusions with high Li/B ratio found from HP/LT type metasediments

YOSHIDA, Kenta^{1*}, HIRAJIMA, Takao¹

¹Graduate School of Sciences, Kyoto University

Recent studies invoked that the variation of peculiar fluid soluble light elements, such as Li, B and Cl, are capable of suggesting generation depths of fluid released in subduction zones (Scambelluri et al., 2004; Marschall et al., 2007). Crush-leached (CL) fluids extracted from quartz (Qz) veins intercalated with metabasites of the Sanbagawa metamorphic belt show high Li and B concentrations, whose Li/B ratios show a positive correlation with metamorphic grade of the host rocks, i.e., from 0.02 for pumpellyite-actinolite facies to 0.27 for eclogite facies (Sengen et al., 2009). Furthermore, CL fluids extracted from three samples of Qz veins (IR04, IR27 and IR28) intercalated with metasediments in proximal to the eclogite mass in the Besshi district show much higher Li/B ratio (0.36-1.99). Yoshida et al. (2011a) reported Li/B ratio of dehydrated fluids derived from tourmaline-free metasediments showing higher values than those expected from metabasites for the same grade, suggesting that Li/B ratio of dehydrated fluids was controlled by the rock types of host rocks.

To inspect other factors controlling Li/B ratio of dehydrated fluids, Qz fabric, microthermometry-Raman spectroscopy of fluid inclusions and hydrochemical facies of CL fluids were investigated for abovementioned three samples with high Li/B ratio.

Qz grains in the veins show foam microstructure with almost no intracrystalline deformation structures, suggesting that their fabrics are formed at high-T and low-differential stress conditions and that they have escaped from the later stage deformation during the exhumation stage of the metamorphic belt.

Each sample contains two or three kinds of fluid inclusion assemblage (FIA) indicating that they suffer multistage fluid activities in their P-T trajectory. IR04 has three kinds of FIA, FIA-04a, -04b and -04c. FIA-04a, composed of high saline aqueous fluid (7.0-8.7 mass% NaCl_{eq}) and CH₄ gas, are arranged at intragranular planes. Rare annular shaped fluid inclusions are observed within FIA-04a, suggesting that the host rock suffered compression after their entrapment. FIA-04b is arranged at intragranular planes, consisting of single/two phase inclusions of CH₄-CO₂-N₂-H₂ fluid. FIA-04c is two phase inclusions, composed of high saline aqueous fluid (8.7-9.5 mass% NaCl_{eq}) and CH₄-N₂ mixed gas. IR27 contains two kinds of FIA, FIA-27a and -27b, arranged at trans/intra granular planes, respectively. FIA-27a is composed of high saline aqueous fluid (5.7-10.5 mass% NaCl_{eq}) and CH₄-N₂ mixed gas. The occurrence of FIA-27b is restricted to the wall-adjacent Qz grains and their sizes are too small to determine the compositions, though part of them are considered to be aqueous fluid. IR28 has two kinds of FIA, FIA-28a and -28b. FIA-28a, arranged at intra/trans granular planes, is composed of CH₄-N₂ mixed gas and no water is detected. FIA-28b is characterized by the arrangement along intra/trans granular planes and composed of low-saline aqueous fluid (0.9-2.2 mass% NaCl_{eq}) and CH₄-N₂ mixed gas, showing irregular shapes with large size (up to ~40 micron).

CL fluid of IR28 shows dominance of HCO₃, which is known as the characteristics of pore fluid in near surface fracture of continental crust (Bucher and Stober, 2010), and is commonly observed in Qz veins showing strongly deformed fabric (Yoshida et al., 2011b). The low salinity of IR28 is also similar to that of later-stage veins (Okamoto et al., 2008), although the timing of entrapment of FIA-28a and 28b still remain unclear. However, textural observation shows FIA-04a was trapped during the prograde stage and FIA-04b, 04c, 27a, could have been trapped during peak stage or the early stage of the exhumation. CL fluids of IR04 and IR27 are dominant in Na-Cl type. These observations suggest that hydrochemical facies of deep fluids and texture and Qz veins are potential signposts looking for the pristine deep fluids.

Keywords: fluid inclusion, Li/B ratio, subduction zone, Sanbagawa belt, Crush-Leach method, eclogite

Effects of Al and Na on mineralogy of silica deposits from hydrothermal fluids

SAISHU, Hanae^{1*}, OKAMOTO, Atsushi¹, TSUCHIYA, Noriyoshi¹

¹Tohoku University

Silica is one of the most dominant components in the Earth's crust, and is characterized by high solubility with respect to water that is sensitive to temperature. An ubiquitous occurrence of the quartz vein in seismogenic depth of the subduction zones implies the importance of the quartz precipitation in fractures on earthquake cycle. However, the mechanism of quartz vein formation is still poorly understood. One of the difficulties is arisen by the fact that silica can precipitate from hydrothermal fluids as metastable polymorphs such as opals. Hydrothermal fluid contains various minor elements derived from the crustal rocks: and thus it is possible that kinetics of silica precipitation is affected by these minor elements. Our previous study (Okamoto et al., 2010) revealed that the mineralogy of silica from pure Si solutions are different from that from impure solutions including minor amounts of Al, Na and K derived from granite.

In this study, we conducted the hydrothermal flow-through experiments at 430 C and 31 MPa to investigate the effect of Al and Na on precipitation of silica minerals. We use a blank vessel for precipitation of silica minerals without rock/mineral substrates. The Si-supersaturated solutions (300-350 ppm, $C_{Si}/C_{Si,Qtz,eq} = 3-3.5$) were prepared by dissolution of quartz at 350 C, and the concentration of Al and Na in the input solution was systematically changed by dissolution of albite at different temperatures. The concentrations of Al and Na in the input solutions range from 0 to 7 ppm, and the atomic ratio of Al and Na were unity that is same as the stoichiometry of albite.

With increasing Al and Na concentration in the input solutions, the dominant silica mineral systematically changes from amorphous silica, cristobalite to quartz. The atomic ratio of difference of Al and Na between input and output solutions, dC_{Al}/dC_{Na} , was 1.06. The modal abundances of individual silica minerals were estimated from XRD spectra by using the internal reference addition method. With increasing Al concentration in the input solution, the modal abundance of amorphous silica monotonically decreases from 100 to 15 wt.%, whereas that of quartz increases from 0 to 82 wt.%. Cristobalite becomes dominant at the intermediate Al concentration (1-3 ppm) in the input solutions. In the experiments with low Al concentrations ($C_{Al} < 3.0$ ppm) in the input solution, the contents of Al₂O₃ and Na₂O of the products (amorphous silica and/or cristobalite) are less than 0.06 wt%, and no systematic relationship between Na and Al content. On the other hand, in the experiments with high Al solution ($C_{Al} > 3.0$ ppm), the products contains Al₂O₃ and Na₂O are contained up to 0.36 wt.% and 0.25 wt.%, respectively. These lines of evidences suggest that Al³⁺ coupled with Na⁺ substituted for Si⁴⁺ in quartz in our experiments.

Natural silica sinters, which form at shallow levels (< 1 km depth) of the crust, are composed mainly of opaline silica (amorphous silica and cristobalite) with lesser amounts of quartz. In contrast, the hydrothermal quartz veins do not contain the relic of other silica polymorphs, except for chalcedony. Such contrasting mineralogy of silica deposits probably reflect the concentration of Al and Na in the solution. Because solubility and morphology of precipitates are quite different between quartz and amorphous silica, the minor amount of Al and Na in the hydrothermal fluids would affects the location and amount of silica deposits at the Earth's crust.

Keywords: Precipitation of silica minerals, Quartz, Aluminum, Sodium, Hydrothermal experiment

Hydrothermal experiments on calcite precipitation via water-rock interaction

MUSHA, Michimasa^{1*}, TSUCHIYA, Noriyoshi¹, OKAMOTO, Atsushi¹

¹Grad. school of Environmental Studies, Tohoku Univ.

Calcite veins are very common within crusts and accretionary prisms. For example, calcite + quartz veins occur ubiquitously in the Shimanto belt. The solubility of calcite decreased with temperature, that is the opposite trend of quartz; and thus how calcite precipitated in the conditions that quartz also occurs is puzzling. Also, the fluid inclusions in the Shimanto veins are composed of CH₄, with exception of CO₂-dominant inclusions found in the southern parts of the Muroto Peninsula, that belongs to the Tertiary Shimanto belt (Lewis, 2000). In spite of its importance, the experimental studies on the calcite precipitation are very limited. Most experiments are carried out under near room temperature and controlled by pH change or synthetic CO₂ saturated fluids (Lee & Morse, 1999), that are far from natural conditions of calcite-vein formation. To best of our knowledge, there are no experimental studies on calcite precipitation under hydrothermal conditions (>100°C).

The purpose of this study is to understand the controlling factors on calcite precipitation under conditions of calcite-vein formation (fluid compositions, P-T conditions, host rock types). The solubility of calcite increases with decreasing temperature or pH, with increasing fluid pressures, and with increasing concentration of NaCl (Ellis, 1963). What is the most controlling factor that enhances the calcite-vein formation at the conditions of the Shimanto belt is unknown. We conducted two types of hydrothermal flow-through experiments for calcite precipitation by (1) temperature change and (2) water-rock interaction at constant P-T. In both experiments, the P-T condition for calcite precipitation is 300 °C and 30 MPa.

In the first experiments, the supersaturated solutions were prepared by dissolution of limestone sand (1-2 mm in size) in the distilled water at 100 °C. In the precipitation vessel, seven limestone substrates (5x5x15 mm) were set along the flow-path. The limestone is composed of fine grained aggregate of calcite (<0.03 mm). The temperature of the precipitation vessel was set to be 300 °C. The fluid flow rate was 2.5 ml/min. After the run of 240 h (10 days), the total increase of weight of limestone substrates was 0.051 g. Observations by SEM and by optical microscope reveal that epitaxial growth calcite from substrate crystals with size of 0.02-0.03 mm.

In the second experiment, we used NaHCO₃ solution (pH 8.4) as input solution. In the preparing vessel, sands of sandstone, mudstone or basalt from the Shimanto belt were set to dissolve Ca and other cations. In the second vessel, four limestone substrates as the same size as the first experiment. The measured fluid flow rate was 2.59 ml/min. After the run of 240 h, the total increase of weight of substrates was 0.037 g. Observation of the surface of the substrates by SEM and EDS reveal that calcite crystals with size of 0.01 mm precipitated together with clay minerals and apatite.

Our results suggest that calcite veins could be formed at high temperature around 300 °C, in higher pH fluids, if fluids saturated with calcite by Ca from host rocks and CO₃²⁻ in the crustal fluids. The possibility of the formation of quartz and calcite vein is also suggested from the precipitation of silicate and calcite from natural rock samples at the same temperature. The source of Ca and CO₃²⁻ would be the host sedimentary or basaltic rocks in the Shimanto belt.

References: Lewis J. C., Byrne T. B., J.D.Pasteris, (2000), *J. metamorphic Geol.*, 2000, 18, 319-333

Y. J. Lee, J. W. Morse, (1999), *Chemical Geology*, 156 (1999), 151-170

A. J. Ellis, (1963), *American Journal of Science*, 261, 1963, 259-267

Keywords: calcite precipitation, crustal fluid, CO₂ storage, Shimanto belt

Thermal history of Earth and the evolution of oceans

KORENAGA, Jun^{1*}

¹Yale University

Our understanding of the thermal budget of Earth and its long-term evolution has been considerably improved in the last several years, owing to an unusual confluence of new theoretical developments and multi-disciplinary observations. In this contribution, I will present the latest summary on the thermal history of Earth during the last 4 billion years and discuss how it may be exploited to better understand the global water cycle and the evolution of oceans. To be consistent with the thermal evolution of Earth, the Archean oceans may have been twice as voluminous as the present-day oceans, and Earth's mantle is suggested to have been gradually hydrated by subduction. Net water exchange between the surface reservoir and the deep interior is likely to be essential for the stable operation of plate tectonics over Earth's history.

A seismic cluster at 155 km depth beneath Niigata: Implications for phase transformation from gabbro to eclogite

NAKAJIMA, Junichi^{1*}, UCHIDA, Naoki¹, Bradley Hacker², HASEGAWA, Akira¹

¹Graduate School of Science, Tohoku University, ²University of California, Santa Barbara

Intermediate-depth earthquakes occur at depths of 60-300 km, forming the double Wadati-Benioff zone in subduction zones as a global prevalence (Brudzinski et al., 2007). Because of high pressures that prohibit brittle failure at such depths, the genesis of intermediate-depth earthquakes has been discussed in terms of dehydration embrittlement (Seno and Yamanaka, 1996; Peacock, 2001; Jung et al., 2004) or periodic shear heating (Kelemen and Hirth, 2007).

We find a tiny seismic cluster in the lower crust of the Pacific plate at a depth of 155 km and analyze it based on waveform similarity. The cluster consists of sub-clusters with similar waveforms, and earthquakes in each cluster lie on single fault plane with complementary rupture areas. This result suggests that earthquake occur as a reactivation of pre-existing hydrated faults. We also reveal that in the cluster, tensional faulting occurs closer to the top of the slab and compressional faulting is dominant away from the slab surface. Since regional stress around the cluster is compression, we interpret that shallow tensional faulting occurs as a result of a stretching deformation in the transformed crust underlain by untransformed crust. Our observations may reflect ongoing gabbro-eclogite transformation at a pressure of ~5 GPa.

Keywords: intermediate-depth earthquake, dehydration, weak fault

Insight into Amphibole-rich mafic-ultramafic rocks beneath island arc: an example from Shikano-shima, Kyusyu, Japan

MORISHITA, Tomoaki^{1*}, Massimo Tiepolo², Antonio Langone², YUHARA, Masaki³

¹Kanazawa Univ., ²CNR-Pavia, ³Fukuoka Univ.

The role of amphibole in arc magma petrogenesis is not completely understood yet. Amphibole might be an important phase of crystallization at middle to lower crustal conditions in arc settings, and therefore might be an important role in the formation of arc magmas (Davidson et al., *Geology*, 2007). Amphibole-rich mafic and ultramafic rocks formed at the deeper part of arc setting are not studied well. Amphibole-rich rocks are commonly observed in the Ryoke belt, Japan, closely associated with granitic rocks (Kamei et al., *Lithos*, 2004; Yuhara & Kagami, *Sci. Rep Fukuoka Univ.*, 2007). We examined petrological and mineralogical characteristics coupled with zircon chronology of amphibole-rich mafic rocks in the Shikano-shima granitic rocks of the Cretaceous age (Yuhara & Uto, *Jour. Geol. Soc. Japan*, 2008). We concluded that older (up to 20 Ma) amphibole-rich ultramafic rocks, which might be related to continental arc magmas, were assimilated by a mafic melt of high-Mg andesite affinity.

Keywords: fluid, amphibole, Island Arc

In-situ electrical conductivity measurement of serpentinite during shear deformation

KAWANO, Seiya^{1*}, YOSHINO, Takashi², KATAYAMA, Ikuo¹

¹Department of Earth and Planetary Systems Science, Hiroshima University, ²Institute for Study of the Earth's Interior, Okayama University

Electrical conductivity anomaly has been found in mantle wedge above subducting slab (Yamaguchi et al., 2009). The subducting slab re-releases most of the water to the mantle wedge by the dehydration reactions, and the expelled water reacts with mantle rocks, forming serpentinite and minor amount of magnetite at the plate interface. Stesky and Brace (1973) reported that some serpentinites have high conductivity of 10^{-2} S/m even at room temperature, and that the others have low conductivity of 10^{-5} S/m. Microstructural observations indicated that the observed high conductivity is caused by the interconnection of magnetite (10^4 S/m) grains, which are produced during serpentinization. However, magnetite distribution and precipitation mechanism should be considered to extrapolate laboratory conductivity data of a few millimeter sized sample to several kilometers geological scale (Watanabe, 2005). Then we inferred that the deformation controls interconnection and orientation of magnetite in serpentinites, because the mantle wedge rocks at the plate interface are subjected to noncoaxial stress and widely develop a strong alignment of constituent minerals. Therefore, we designed experimental cell for the electrical conductivity measurement of during shear deformation, and discuss here the influence of strain and magnetite volume fraction on connectivity of magnetite.

The electrical conductivity measurements of serpentinites with various amount of magnetite were conducted using an impedance analyzer under high pressure generated by a cubic anvil apparatus. The electrical conductivity of serpentinites was investigated in the frequency range of 10^1 -106 Hz and temperature range of 500-750 K at 1 GPa along the shear direction. Starting materials were powder mixture of serpentine and magnetite. The mixed samples were sintered in a piston cylinder apparatus at 1GPa and 500°C. The sintered materials were prepared to be 2 - 3 mm length and 0.8mm^2 of cross-section area. (2.0 mm by 0.4 mm). The serpentinite sample was sandwiched between alumina pistons which were cut at 45° from the maximum compression direction. Ni electrodes for the electrical conductivity measurement were placed at each side of sample and played a role as strain marker to assess the strain from rotation of boundary between sample and Ni. In shear deformation experiment, deformation rate was fixed to be 200 micrometer per hour for 8 hours.

We measured the electrical conductivity during heating from 500 K to 750 K. The conductivity values of the serpentinite were 10^{-3} to 10^{-2} S/m. In all experiments, logarithmic conductivity linearly increased and decreased with increasing and decreasing reciprocal temperature, and we obtained systematic results against volume fraction of magnetite. During shear deformation, electrical conductivity increased with increasing strain. Activation energy did not change each samples before and after deformation.

The result showed that only the data of 20 vol. % magnetite content reach into value of conductivity anomaly in mantle wedge. It is difficult to explain electrical conductivity anomaly by deformation of natural serpentinite, because magnetite content of natural serpentinite is generally less than 5 vol. %. Therefore a presence of free aqueous fluid with seawater-like composition would be required to explain high conductivity anomaly observed in the mantle wedge.

Keywords: Electrical conductivity, Serpentinite, Subduction zone, in-situ measurement, Magnetite

Seismic velocities of serpentinites - Influence of geometry of antigorite grains

WATANABE, Tohru^{1*}, SHIRASUGI, Yuto¹, MICHIBAYASHI, Katsuyoshi²

¹University of Toyama, ²Shizuoka University

Serpentinites play key roles in subduction zone processes including transportation of water, seismogenesis, slab-mantle coupling, and exhumation of high-pressure rocks. Geophysical mapping of serpentinitized regions leads to further understanding of these processes. Direct study of serpentinites is critical to the interpretation of indirect geophysical observations.

Determination of elastic constants of antigorite (Bezacier et al., 2010) has enabled us to calculate Voigt and Reuss bounds of seismic velocity in serpentinites. There is, however, considerable difference between two bounds due to strong elastic anisotropy of antigorite. Seismic velocity in serpentinites cannot be properly constrained by these bounds that consider mineral composition and orientation of crystal grains. Geometry of antigorite grains (thin plate), which is not considered in Voigt and Reuss bounds, should be taken into account for a better constraint (Watanabe et al., 2011).

We calculated seismic velocity in serpentinites by using a differential effective medium method (DEM). An antigorite grain is treated as a spheroidal inclusion, and embedded in a homogeneous matrix. Strain in the matrix are disturbed by introducing an inclusion, and evaluated by Eshelby's method. Elastic constants of the composite material can be calculated by differentiating the elastic energy with respect to strain. Nishizawa and Yoshino (2001) calculated seismic velocity in mica-rich rocks by embedding spheroidal inclusions with an identical orientation in an isotropic matrix. We modified their method and applied it to the case where spheroidal inclusions with different orientations are embedded in an anisotropic matrix.

Decreasing aspect ratio of an spheroidal inclusion, seismic velocity in serpentinites decreases and approaches to Reuss bound. When spheroidal inclusions are aligned, seismic anisotropy is enhanced with smaller aspect ratio. Seismic velocity calculated by using orientations of crystal grains reasonably reproduces that measured in laboratory. The velocity calculation considering the geometry of antigorite grains is promising for a good prediction of seismic velocity in serpentinites.

Keywords: seismic velocity, serpentinite, serpentine, antigorite, water, subduction

Microseismic-based detection of fluid flow in deep seated rock and its application to geothermal development

ITO, Takatoshi^{1*}

¹Institute of Fluid Science, Tohoku Univ.

In the hydraulic stimulation, massive fluid is injected into subsurface rock through drilled wells. Then a number of microseismic events are commonly observed. By analyzing those data of microseismic events, we can estimate the orientation, i.e. dip and strike, of the fracture which slips to induce microseismic event. From the estimated fracture orientation, taking into account the in situ stresses and the Mohr-coulomb criterion to describe the critical condition of fracture slipping, we can estimate the pore pressure at the location of slipping fracture and at the time when the slipping occurs, in other words, when the microseismic event occurs. The estimated values of pore pressure are sorted in a certain manner for each equally divided spatial region, i.e. block, to give spatial distribution of pore pressure and its variation with time during hydraulic stimulation. We applied this method to the microseismic data observed during the hydraulic stimulation performed in November 2003 at the HDR development site of Cooper Basin in Australia, and we succeeded in showing the pressure propagation through the rock formation during the test.

Keywords: Fluid flow, Microseismicity, Coulomb criteria, Inverse problem, Hydraulic fracturing, Geothermal development

Hydrothermal alteration in the Caleta Coloso fault core zone of the Atacama Fault System, Chile

FUJITA, Kazuna¹, Rodrigo Gomila², Jose Cembrano², HOSHINO, Kenichi^{1*}

¹Grad. Sch. Sci., Hiroshima Univ., ²Dept. Struct. Geotech. Eng., Pontificia Univ. Catolica de Chile

The Atacama Fault System (AFS) is a trench-parallel large-scale structure developed within mesozoic rocks of the present-day Coastal Cordillera in northern Chile (Cembrano et al., 2005). Its well-documented left-lateral activity has been interpreted as the result of the SE-ward oblique subduction of the Aluk (Phoenix) oceanic plate between 190 and 110 Ma (e.g., Schuber and Gonzalez, 1999). Recent activity of the AFS has been documented mainly as extensional and interpreted as a reactivation of the system in response to mega-thrust earthquakes (e.g., Gonzalez et al., 2006).

The Caleta Coloso Fault of the AFS is represented as a N-S to NNW-SSE west-ward concave-shape sinistral strike-slip fault showing a left-lateral displacement of about 3 km and a subvertical dip (Cembrano et al., 2005). The fault cuts through crystalline rocks of predominantly granodioritic composition (Gonzalez and Niemeyer, 2005) and its fault core currently displays hydrothermally altered cataclastic rocks (Olivares, 2004).

Two types of hydrothermal alteration, chloritization and propylitization, can be observed in the Caleta Coloso fault core zone. The former is characterized by the replacement of hornblende and biotite by chlorite, epidote mineralization and compositional changes in rims of plagioclase to albite-rich ones, while the latter by the intense plagioclase albitization and mineralization of chlorite, epidote and calcite. XRF analyses and density measurements of the rock revealed that contents of Al and Ca decrease with increasing Si, while Na increases and K, Fe and Mg are stable. The data suggest that the changes in the bulk chemical composition during alterations were mostly due to the plagioclase albitization. Hence, it can be concluded that the propylitization occurred later than the chloritization.

Faulkner et al. (2006) reported that the density of microfractures shown as fluid inclusion planes (FIPs) in quartz of the host rocks of the Caleta Coloso fault increases towards the fault core. Fujita et al. (2010) also noted that the FIPs in the rocks close to the fault tend to orientate along the shear planes (Y and P planes and between T and X planes of the fault). Those evidences indicate that the microfractures were formed during faulting and healed by mineral precipitation from fluids passing through the fractures and that the fluids have been preserved as the fluid inclusions in FIPs (Fujita et al., 2010).

The fluid inclusions in the chloritized rocks show a wide range in homogenization temperatures from 140 to 270 C with variable salinities of 6 - 18 wt.% NaCl_{eq.}, while the temperatures of those in the propylitized rocks are low as 150 - 190 C (av. = 170 C) with high salinities as 12 - 18 wt.% (av. = 15 wt.%). Therefore, the fluid inclusions trapped in the both alterations stages are probably included in the chloritized rocks partly overprinted by the later propylitization. However, since the fluid inclusions of only low-homogenization temperatures with high salinities can be seen in the highly propylitized rocks, the most propylitization might completely alter the chloritized rocks with the intense albitization, resulting in removal of older fluid inclusions trapped during the earlier chloritization. Hence, it is supposed that the fluids of high-homogenization temperatures (ca. 250 C) and low salinities (ca. 9 wt.%) caused the chloritization, while those of low-homogenization temperatures (ca. 170 C) and high salinities (ca. 15 wt.%) did the propylitization.

Chemical compositions of chlorite coexisting with quartz indicate the chloritization temperature as around 330 C. A pressure at 330 C on an isochore for the 9 wt.% NaCl solution projected from the homogenization temperature of 250 C is about 1.1 kb, representing the chloritization pressure. Therefore, the propylitization temperature might be around 220 C if the propylitization occurred at the same depth with the chloritization.

Keywords: fault, fluid inclusion, hydrothermal alteration, chloritization, propylitization

The physicochemical reaction during the coseismic-interseismic period of the fault gouge of the MTL, Japan

MATSUTA, Noriko^{1*}, ISHIKAWA, Tsuyoshi², HIRONO, Tetsuro¹, KAWAMOTO, Kazurou³, FUJIMOTO, Koichiro⁴, KAMEDA, Jun⁵, NISHIO, Yoshiro²

¹Earth and Space Science, Osaka Univ., ²JAMSTEC Kochi, ³Oshika Geological Museum of Japan MTL, ⁴Tokyo Gakugei Univ.,

⁵Department of Earth and Planetary Science Graduate School of Science, The University of Tokyo

Frictional heating during coseismic slip induces transient fluid-rock interaction and fluid transfer. It is crucial to understand these physicochemical process and mechanism because these fluids strongly influence the dynamic behavior and rupture propagation of earthquakes. In order to understand these reactions, we investigated the Median Tectonic Line (MTL), which runs through Nagano prefecture and is newly exposed around the Anko outcrop. We performed geochemical analyses of major- and minor-element concentrations, Sr isotope ratio and semi-quantitative clay mineral composition. Using the fluid-mobile trace element spectrum, which is sensitive to fluid-rock interaction at high temperatures, we estimated that the black gouge experienced frictional heating of approximately 150-200 degree Celsius. The clay collected from this black gouge show a distinctly low XRD pattern compared to the surrounding gouge, which may suggest amorphusization of clay minerals related to the shear slip. So the temperature signal probably indicates that frictional heating have occurred in the gouge together with high amount of coseismic fluid transfer.

Detection of deep fluid using lithium isotope of waters along the Atotsugawa fault system, central Japan

OOHASHI, Kiyokazu^{1*}, NISHIO, Yoshiro², TANIKAWA, Wataru³, YAMAGUCHI, Asuka⁴

¹Graduate School of Science, Chiba University, ²Agency for Marine-Earth Science and Technology, ³Japan Agency for Marine-Earth Science and Technology, Kochi Institute for Core Sample Research, ⁴Department of Earth and Planetary Science, The University of Tokyo

The Atotsugawa fault system, central Japan is one of the active faults located in the Niigata-Kobe tectonic zone (strain-concentration zone) which detected dense GPS observation network (Sagiya et al., 2000). Along this fault system, active microearthquakes and possible fault creep has been detected from seismic observations and EDM/GPS survey, respectively (Tada, 1998; Ohzono et al., 2011). However, mechanism for strain concentration along this zone is still open question. Iio et al. (2002) speculated that the dehydrated fluid (water) from the Philippine Sea plate and the Pacific plate may weaken the lower crust beneath the Niigata-Kobe tectonic zone. Recent geophysical observations revealed existence of low resistivity and low velocity bodies beneath the zone (Yoshimura et al., 2009; Nakajima et al., 2010) which is consistent with Iio et al. (2002). Nevertheless, there is no direct evidence to represent existence of water (H₂O), and details about fluids such as origin are still unknown. On the other hand, geochemical signal of ground water can be a reliable evidence for detection of deep fluids if they come up to the shallow portion of the crust. Lithium (Li) is a fluid-mobile element having two stable isotopes, ⁷Li/⁶Li. Amount of Li leached from rock to fluid drastically increases with the temperature, and once leached Li is kept in fluid while decreasing temperature (cooling). These features indicate that Li has a great potential for tracer of deep fluid provide information on the origin and nature of fluid circulation. We thus collected water along the fault system (especially for the water leaking from fault zone), river water and spring water nearby the fault system, and analyzed their chemistry and isotope.

The results show that the several water samples collected from the fault zone have high concentration of Li and significantly lower value of ⁷Li/⁶Li whereas the river water and spring water shows low Li concentration and high ⁷Li/⁶Li value. These results suggest that the deep-crustal fluid which has peculiar chemical properties exists beneath the Atotsugawa fault system, and upwelling to the ground along the fault zones.

[References]

Iio et al., 2002, *Earth planet Sci. Lett.*, 203, 245-253.

Nakajima et al., 2010, *Earth Planets Space*, 62, 555-566.

Nishio et al., 2010, *Earth planet Sci. Lett.*, 297, 567-576.

Ohzono et al., 2011, *Geophys. J. Int.*, doi:10.1111/j.1365-246X.2010.04876.x.

Sagiya et al., 2000, *PAGEOPH*, 157, 2303-2322.

Tada, 1998, *Chikyu*, 20, 142-148.(in Japanese)

Wada et al, 2007, *Disaster Prevention Research Institute annuals*, 50, 313-320.(in Japanese)

Yoshimura et al., 2009, *Geophys. Res. Lett.*, 36, L20311, doi:10.1029/2009GL040016.

Keywords: Atotsugawa fault, Niigata-Kobe Tectonic Zone, geofluid, lithium isotope, fault fluid, Intraplate earthquake

Trace elements and isotopic variations along Sunda arc, Java island, Indonesia: an evaluation of slab fluid contribution

HANDINI, Esti^{1*}, HASENAKA, Toshiaki¹, Haryo Edi Wibowo¹, SHIBATA, Tomoyuki², Yasushi Mori³, HARIJOKO, Agung⁴

¹Graduate School of Science and Technology, Kumamoto University, ²Beppu Geothermal Research Laboratory, Kyoto University, ³Kitakyushu Museum of Natural and Human History, ⁴Department of Geological Engineering, Gadjah Mada University

A geochemical dataset of lavas from Java island, Sunda arc is compiled for trace elements and isotopic variations, in order to understand along-arc variation of the contribution of slab-derived fluid to arc magmas. We divided the island into western, central and eastern sections in terms of volcanism and tectonics. Based on volcano distribution, the western section is subdivided into North-West Java (NWJ) and Central-West Java (CWJ) chains. The NWJ chain is considered to be tectonically affected by bending subduction structure that marks the transition from Sumatra arc to Sunda arc.

In general, lavas from this island are distinguished by enriched LILE and LREE, negative anomalies of Nb and Ti, and low Mg, Ni and Cr. We observed along-arc variation of subduction slab imprint including both sediment (SED) and altered oceanic crust (AOC) by examining fluid-mobile elements against HFSE ratios (e.g. B/Nb, B/Zr, Ba/La). We also evaluate depletion of Nb which characterizes arc magmas, by using Nb/HFSE (e.g. Nb/Ta, Nb/Zr) ratios, along this island. Radiogenic Sr-Nd isotopes were determined to examine contribution of SED and AOC to arc magma source. Then we combine these to find differences between western, central and eastern sections.

Nb/HFSE ratios are evenly low along western, central and eastern sections. However, these ratios increase from volcanic front toward back arc in central and eastern sections. In contrast, they are uniformly low across the western section, with little deviation in NWJ chain. The B/HFSE and Ba/HFSE ratios decrease from volcanic front toward back arc in the central and eastern sections. Whereas, they decrease but slightly across the western section. They are observed highest in lavas from central section compared to others. Isotopic ratios from all sections are shifted from Indian Ocean MORB field toward higher ⁸⁷Sr/⁸⁶Sr and lower ¹⁴³Nd/¹⁴⁴Nd ratios. Back-arc lavas from central section overlap with mantle array and exhibit the lowest ⁸⁷Sr/⁸⁶Sr in a wide range of ¹⁴³Nd/¹⁴⁴Nd ratios, whereas the volcanic-front samples overlap with compositions of Indian Ocean sediment. Back arc lavas from eastern section are displaced toward sediment composition, while the volcanic front is placed closer to MORB.

This increasing trend of Nb/HFSE from volcanic front toward back arc in central and eastern sections implies more enriched mantle source in the back arc. This back arc source enrichment is then confirmed by isotopic ratios. Despite the little deviation in NWJ chain, the general flat trend as observed in western section indicates similar mantle source across this section. Positive correlation between incompatible elements ratio and the depth of Wadati-Benioff zone denotes an identifiable influence of subducted slab along this island. The sharp decreasing trends of B/HFSE and Ba/HFSE in central and eastern sections suggest a definite reduced slab-fluid influence from volcanic front toward back arc. Compared to these sections, the western section is less pronounced in terms of subduction components enrichment. The greatest enrichment of subduction components in central section implies strongest slab fluid imprint in this section. The Sr-Nd isotopic pattern justifies the involvement of slab fluid in all sections. However, this pattern confirms the strongest subducted sediment-fluid contribution in volcanic front of central section. The more enriched mantle source in back arc compared to volcanic front is observed in eastern section. This evidence corroborates mantle source enrichment towards the back arc, in central and eastern sections.

Keywords: sunda arc, along arc variation, slab fluid, fluid-mobile element, isotope

Geochemical tomography for melting condition beneath Japan arcs

NAKAMURA, Hitomi^{1*}, IWAMORI, Hikaru¹

¹Tokyo Institute of Technology

Slab-derived fluid (hereafter slab-fluid) plays an important role for generation of arc magmas. If the flux of slab-fluid is enhanced or reduced by variable tectonic settings and the corresponding thermal and flow regimes, it has effects on the mantle melting. The melting condition may contribute to infer the thermal, flow and fluid regimes. We focus on the melting condition in the mantle wedge beneath Central Japan, where the two overlapping slabs, Pacific and Philippine Sea plates, exist and the amount and composition of slab-fluids from the two slabs are well documented, as the regional variation of slab-fluid fluxes that are related to the geometry of the subducting plates.

Based on the chemical composition of major and trace elements, we construct forward and backward models to constrain the melting condition beneath Central Japan. The composition of the primitive rock can be corrected for fractionated phases to estimate backwardly that of primary magma, while the composition of melt generated in the mantle wedge can be forwardly modeled as a function of degree of melting (sensitive to temperature) and mineralogy (proportions of garnet/spinel peridotites, sensitive to pressure) based on the composition of fluid metasomatized mantle.

As a result, the melting condition is characterized by relatively low melting degrees and high proportions of garnet peridotite involved in melting compared to the adjacent arcs with a single subducting slab, e.g., the Izu-arc. This implies that, the melting occurred at deeper depths and lower temperature for Central Japan. This also consistently explains the existence of adakites occurred in this area, in spite of the cold setting. The same analysis for the volcanoes in the adjacent areas show transition the thermal and fluid conditions, according to the spatial variation of the tectonic regimes, suggesting that geochemical approach is useful to map the physical condition, and could be referred to as geochemical tomography.

Keywords: mantle, melting, slab, slab-fluid, subduction, arc

Experimental constraints on partitioning of hydrogen between plagioclase and basaltic melt

HAMADA, Morihisa^{1*}, USHIODA, Masashi¹, TAKAHASHI, Eiichi¹

¹Department of Earth and Planetary Sciences, Tokyo Institute of Technology

Introduction: The hydrogen in nominally anhydrous minerals (NAMs) can be an indicator of H₂O activity in silicate melts if the partitioning behavior of hydrogen between NAMs and melts is known. Plagioclase is one of the NAMs and one of the most common minerals in arc basaltic rocks. Therefore, hydrogen in volcanic plagioclase (OH) can be a useful proxy of H₂O in arc basaltic magmas. Here, we report experimental results on the partitioning of hydrogen between Ca-rich plagioclase and basaltic melt. We also apply the OH concentration of plagioclase as hygrometer of melt based on experiments.

Experimental: Hydrous melting experiments of arc basaltic magma were carried out at 350 MPa using an internally-heated pressure vessel installed at Magma Factory, Tokyo Institute of Technology. Starting material was hydrous glass (0.8 wt.% <H₂O<5.5 wt.%) of an undifferentiated rock from Miyakejima volcano, a frontal-arc volcano in Izu-arc (MTL rock: 50.5% SiO₂, 18.1% Al₂O₃, 4.9% MgO). A grain of Ca-rich plagioclase (about 1 mg, An₉₅, FeO_t = 0.4 wt.%) and 10 mg of powdered glasses were sealed in Au₈₀Pd₂₀ alloy capsule, and then kept at around liquidus temperature. Liquidus phase of MTL rock at 350 MPa is always plagioclase with 0 to 5.5 wt.% H₂O in melt (Ushioda, unpublished data), and therefore, a grain of plagioclase and hydrous melt are nearly in equilibrium. Oxygen fugacity (*f*O₂) during the melting experiments was not controlled, and the intrinsic *f*O₂ of the pressure vessel was estimated to be 3 log unit above Ni-NiO buffer. Experiments were quenched after 24-48 hours, long enough to attain equilibrium partitioning of hydrogen between plagioclase and melt. Concentration of H₂O in melt (both molecular H₂O and OH) and concentration of OH in plagioclase was analyzed by infrared spectroscopy.

Results: Experimental results are summarized in Fig. 1. Correlation between total H₂O (molecular H₂O and OH) concentration in melt and OH concentration in plagioclase is non-linear: partition coefficient in molar basis is about 0.01 with low H₂O in melt (< 1 wt.%), while it decreases with increasing H₂O in melt (Fig. 1a). The OH concentration of plagioclase reaches 200-250 wt. ppm H₂O with > 4 wt.% H₂O in melt and saturates. OH in plagioclase linearly correlates with OH in melt (Fig. 1b), which confirms that hydrous species in plagioclase is OH ion as suggested by previous studies.

Application: The OH concentration of Ca-rich plagioclase (about An₉₀) from the 1986 summit eruption of Izu-Oshima volcano, also a frontal-arc volcano in Izu-arc, shows variation ranging from <50 wt. ppm H₂O through 300 wt. ppm H₂O as a result of polybaric degassing (Hamada et al., 2011, EPSL). Hamada et al. (2011) claims that pre-eruptive melt dissolves H₂O up to 6 wt.% and that melt undergoes polybaric degassing during ascent and eruption, based on (i) variation of OH in plagioclase, (ii) hydrous melting experiments to crystallize An₉₀ plagioclase, and (iii) geophysical observation of the 1986 summit eruption of Izu-Oshima volcano. In consistent with previous studies, this experimental studies demonstrates that plagioclase with >250 wt. ppm H₂O can be in equilibrium with melt dissolving >4 wt.% H₂O (Fig. 1a). Such high H₂O concentration corresponds to saturated H₂O concentration in melt at 8 to 10-km-deep magma chambers beneath Izu-Oshima volcano (Mikada et al., 1997, PEPI). Plagioclase from the 1986 summit eruption of Izu-Oshima volcano is expected to record polybaric degassing history of H₂O-saturated magma during eruption.

Keywords: Water in nominally anhydrous minerals, plagioclase, arc basaltic magma, hydrous melting experiment

SCG65-P02

Room:Convention Hall

Time:May 20 17:15-18:30

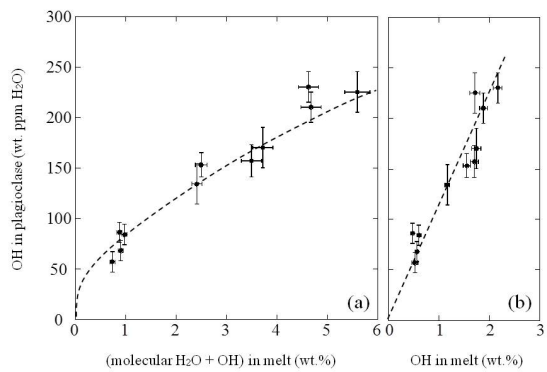


Fig. 1

What stays in the slab and what returns to the surface? A geochemical mass balance model perspective

KIMURA, Jun-Ichi^{1*}, KAWABATA, Hiroshi¹, Bladley Hacker², Peter van Keken³, James Gill⁴, Robert Stern⁵

¹IFREE/JAMSTEC, ²University of California, Santa Barbara, ³University of Michigan, ⁴University of California Santa Cruz, ⁵University of Texas at Dallas

We have developed the Arc Basalt Simulator (ABS), a quantitative forward model to calculate the mass balance of slab dehydration and melting, and slab fluid/melt-fluxed mantle melting, in order to quantitatively evaluate magma genesis beneath arcs. ABS models can reproduce magma compositions in many arcs.

The model suggests that the slab-derived component at volcanic fronts (VF) is mostly generated by dehydration, but successful models for most VF and all rear arc (RA) magmas also require the slab to melt. The compositions of slab fluids and melts are controlled primarily by the breakdown of amphibole and lawsonite beneath the VF and by the breakdown of phengite beneath the RA in addition to residual eclogite mineral phases including garnet, clinopyroxene, and quartz.

In the model, about 78-98% of relatively fluid-immobile elements including Nd and Hf in the arc lavas come from mantle peridotite. However, most liquid-mobile elements come from the slab. Modeled residual peridotite compositions are similar to those in some supra-subduction zone ophiolites and mantle xenoliths, providing constraints on reactions in the mantle wedge.

Altered oceanic crust (AOC) and sediment in the residual slab are modified by the subtraction of melt- and fluid-mobile elements. Unmodified AOC potentially becomes the EM I mantle component after 1 Ga, whereas melted AOC can have extremely fractionated U-Pb and become the HIMU source after 1-2 Ga. Element re-distribution beneath arcs can form the recycled materials that have been detected in ocean island basalts.

Keywords: arc, magma, geochemistry, mass balance

Pb isotopic compositions of hydrothermal deposits in the Japanese island arc

FUJINAGA, Koichiro^{1*}, KATO, Yasuhiro¹, HIEDA, Yuki¹, TAKAYA, Yutaro¹, Masaharu Tanimizu², SHIMIZU, Toru⁴, NAKAMURA, Hitomi³, IWAMORI, Hikaru³

¹University of Tokyo, ²JAMSTEC, ³Tokyo Institute of Technology, ⁴Geological Survey of Japan

Quite recently, it has been pointed out that "geofluids" released from the subducting plates may be involved in various phenomena in subduction zone, such as young volcanic rocks, deep-seated hot springs and hydrothermal deposits. Systematical investigations of these various materials are needed for identifying the geochemical characteristics of the geofluids. Nakamura et al. (2008) revealed that the slab-fluids derived from two subducted plates (the Pacific plate and the Philippine Sea plate) contribute largely to the genesis of arc magmas in the Central Japan. Here we focus on hydrothermal deposits (vein-type and skarn-type) in the Japanese island arc. Hydrothermal fluids that formed sulphide mineral (galena, pyrite, chalcopyrite, sphalerite etc.) deposits are generally considered to have been derived from magmatic and/or meteoric waters based on H, C, O, and S isotopes in the deposit materials. However, ore fluids may be derived from deep slab-fluids. We report Pb isotopic compositions of hydrothermal deposits in the Japanese island arc and discuss about the origin of ore fluids.

Keywords: Pb isotopic composition, hydrothermal deposit, slab-fluid

Rare earth element composition of the Arima-type brine and its implication for slab-derived fluid

YOSHIYUKI, Fujita^{1*}, NAKAMURA, Hitomi¹, KUSUDA, Chiho², IWAMORI, Hikaru¹

¹Department of Earth and Planetary Sciences, Tokyo Institute of Technology, ²Department of Earth and Planetary Science, The University of Tokyo

The Arima-type brine has been known as one of the oldest hot springs in Japan, as well as its distinct geochemistry: in spite of its presence in the non-volcanic region in the forearc, the oxygen and hydrogen isotope compositions show a presence of deep brine similar to volcanic fluids. Mixing between the meteoric water and a deep brine with a high $\delta^{18}\text{O}$ and $\delta^2\text{H}$ (7 to 8, -40 to -30, respectively) explains the linear trend of the brine samples. The Arima-type brines are highly concentrated in the type locality, Arima, SW Japan. The two plates subduct beneath the area: the Pacific Plate subducts from the east and underlies ~400 km below the area, whereas the Philippine Sea Plate subducts from the southeast and is seismically observed 50 to 80 km below the area. In spite of this active subduction, there is no Quaternary volcano in this area, possibly because the Pacific Plate is too deep and the Philippine Sea Plate is too shallow to fulfill the physicochemical conditions for arc magma generation.

Here we report geochemical signatures, in particular the REE concentrations, of the Arima brine, and suggest that it could have originated directly from the subducting slab without any significant modification during its ascent. High salinity, high $^3\text{He}/^4\text{He}$ ratio and distinct oxygen, hydrogen and carbon and strontium isotope compositions also suggest that they have been derived possibly from the subducting Philippine Sea slab, hence may bring invaluable insights for the slab-derived fluid and the related fluid processes in subduction zones. In this study, we analyzed samples from 'Kinsen'. The Kinsen brine has a high salinity and the highest abundances of the trace elements in this area. We have also sampled a solid material precipitated within the pipe, in order to estimate the elemental fractionation during cooling of the hot spring and precipitation from it. Because of its high salinity (up to 6 wt.% NaCl) of the Arima-type brine, the matrix effects are extremely large to prevent accurate analysis of any trace element. We employ a standard addition method, aiming at rapid yet accurate analyses.

The DMM normalized composition of Arima brine exhibits broadly a flat pattern around the normalized concentration of 10-3 with a convex-down shape for mid-REE, except for positive anomaly in Eu. On the other hand, the precipitates consist of aragonite and magnesite, which do not contain REE above the detection limit, except for Gd which is likely derived as flakes from the pipe.

Alternatively, based on the reported partition coefficient and the numerical modeling of the thermal structure along the subducting slab, the REE concentrations in the slab-derived fluid (as a product of slab dehydration reactions) have been evaluated. The calculation results broadly coincide with the observed REE concentrations of the Arima-type brine. Together with these analytical results and forward calculation, we conclude that the REE composition in the Arima brine is straightly originated from the dehydration of subducting slab at 450 degree.

Keywords: slab-derived fluid, Arima brine, rare earth elements, isotopic compositions of oxygen and hydrogen, Arima-type brine, subduction zone

Two-stage serpentinization reactions: an example of Iwanai-dake ultramafic rocks, Kamuikotan belt, Hokkaido, Japan.

MIYOSHI, Akane^{1*}, KOGISO, Tetsu¹

¹Human and Environmental Studies, Kyoto University

The transformation of ultramafic rocks to serpentinites is an important process that influences geodynamic systems in subduction zones. Serpentinization changes physical properties of mantle peridotite. Furthermore, serpentinization in subduction zone affects water and material circulation and mantle dynamics. Despite this renewed interest in serpentinization, the underlying peridotite-water reactions are poorly understood. In recent years, a two stage model for serpentinization has been proposed. Serpentinization generally produces a large amount of magnetite, and petrography and magnetic properties of serpentinite show that magnetite is formed at the later stage of serpentinization. For example, Bach et al. (2006) proposed the formation of magnetite during the breakdown of brucite. On the other hand, Frost and Beard (2007) proposed the breakdown of ferroan serpentine under low silica activity condition. In addition to these, various reactions have been proposed. Although magnetite is an important factor that affects density or magnetic susceptibility of rocks, the previous studies didn't show enough petrographical evidence that support for the reactions proposed. In this study, serpentinization processes of Iwanai-dake peridotite, Kamuikotan belt, Hokkaido, have been investigated with petrological observations, chemical analyses, measurement of density and magnetic susceptibility. On the basis of these data, we discuss chemical processes that are responsible for magnetite formation.

The Iwanai-dake ultramafic body is located in the southern part of Kamuikotan belt, Hokkaido, Japan. A fresh peridotite body, which is about 1 km diameter, is located at the top of Mt. Iwanai-dake. It comprises harzburgite with a small amount of dunite. Ultramafic rocks surrounding peridotite are partly or completely serpentinized. Textures and mineral assemblages were identified by petrographic observation, and Raman spectroscopy. Mineral composition was determined by SEM-EDS. The serpentinite samples mainly consist of serpentine, brucite, and magnetite. Serpentine shows typical mesh textures. There are two kinds of mesh rim types in this area: Type A (Mg#97 serpentine and Mg#75 brucite) and, Type B (Mg#93 serpentine). Type B is associated with Mg#90 brucite vein in the central part. In harzburgite, with progress of serpentinization, mesh rim texture changes from Type A to Type A+B, and Type B only. Type B is always associated with serpentinization of orthopyroxene. Type B and Mg#90 brucite vein are not observed in dunite. The magnetic susceptibility of harzburgite increases rapidly with increasing amount of serpentine, but that of dunite remains low. It is shown that magnetite appear only high-serpentinized harzburgite.

These observations show that the serpentinization proceeded as follows: First, Mg#95-97 serpentine and Mg#75 Brucite were formed by isochemical reaction of olivine-H₂O. Second, Mg#93 serpentine (and Mg#90 Brucite vein) was formed. The second stage reaction was caused by addition of SiO₂ rich fluid from serpentinization of orthopyroxene, as evidenced by no observation of the second stage reaction in dunite sample. Relation between magnetic susceptibility and density shows that magnetite was formed at the second-stage serpentinization. It is thought that the supply of SiO₂ was the trigger of the formation of magnetite. The result differs from the proposal of Frost and Beard (2007). However, the textural classification in this study is inapplicable to the texture discussed by Bach et al. (2006). It is necessary to consider that serpentinization depends on tectonic setting, chemical component of fluid, or mineral assemblage of protolith.

References: Bach, W., H. Paulick, C. J. Garrido, B. Ildefonse, W. P. Meurer, and S. E. Humphris (2006), *Geophys. Res. Lett.*, 33, L13306, doi:10.1029/2006GL025681. ; Frost, B. R. & Beard, J. S. (2007). On silica activity and serpentinization. *Journal of Petrology* 48, 1351-1368.

Cl-bearing CO₂-H₂O fluid-inclusions of peridotite xenoliths from Ichinomegata

KUMAGAI, yoshitaka^{1*}, Tatsuhiko Kawamoto¹, Junji Yamamoto¹

¹Inst. Geothermal Sci., Kyoto Univ.

Hydrous minerals in a subducting slab carry OH- and H₂O into the Earth's interior, and at points beyond their stability conditions they release H₂O to the overriding mantle wedge (Tatsumi and Eggins 1995). The H₂O fluids transport materials from the slab to the mantle wedge. Recently, analyses of halogen elements of high-pressure metamorphic rocks suggest that saline fluids are preserved in the subducting slab as marine pore-fluids until the depths of at least 100 km (Sumino et al., 2010, EPSL). Salinity of H₂O fluids affects dissolution properties of metal ions (Keppler, 1996, Nature). It is, therefore, important to understand the salinity of the H₂O fluids in the mantle wedge in terms of subduction system of metal.

Fluid inclusions in mantle xenoliths preserve direct information of the fluids in the mantle. Mantle xenoliths from the Ichinomegata volcano, located in back-arc side in the northeast Japan arc, have CO₂-H₂O fluid inclusions (Roedder, 1965, Am Mineral). In the present study, we report salinity of the CO₂-H₂O fluid inclusions in the mantle xenoliths from the Ichinomegata volcano.

All mantle xenoliths studied are porphyroclastic lherzolite, composed of olivine, orthopyroxene, clinopyroxene, spinel and hornblende. The CO₂-H₂O fluid inclusions are occasionally present in orthopyroxene porphyroclasts. The fluid inclusions have not reacted with host orthopyroxene crystals after the formation. We suppose, therefore, that the salinity of the fluid inclusions represents the original value in the mantle. Formation depths of the fluid inclusions are estimated by the following steps: (1) estimating the bulk mole volume of CO₂-H₂O fluid inclusion using homogenization temperatures of CO₂ liquid-vapor and CO₂-H₂O (Bakker and Diamond, 2000, *Geochem. Cosmochim. Acta*), (2) calculating pressure of the formation of the fluid inclusion using equilibrium temperature estimated by a pyroxene geothermometer (Wells 1977, *Contrib.Mineral. Petrol.*) and isochore of CO₂-H₂O system (Loner AP, from Software Package FLUIDS, v.2, Bakker), (3) converting the pressure to depth by assuming densities of crust and mantle are 2.85 and 3.3 g/cm³, respectively, and Mohorovicic discontinuity is 27 km. Salinities of fluid inclusions are determined using melting temperature of clathrate (Darling, 1991, *Geochim. Cosmochim. Acta*). The depth is estimated to be about 30 km, which is consistent with the following petrographical feature. Some xenoliths have plagioclase and symplectites formed by reaction of plagioclase and olivine. This indicates that the xenoliths were from the boundary between plagioclase-peridotite and spinel-peridotite. The salinity of fluid inclusions is 3.93 ± 0.55 wt %. Using relationship between the molinity of Cl and the fluid/melt partition coefficients (Zajacz et al., 2008, *Geochem. Cosmochim. Acta*), for example, the fluid/melt partition coefficients of Pb and Zn under this salinity are 7.8 and 18.6, respectively (those of Cl-free hydrous fluid are almost 0 and 8.2, respectively).

Keywords: salinity, fluid inclusion, material transport, subduction zone, mantle xenolith, Ichinomegata

Numerical simulations of temperature distributions associated with subduction of the plate beneath Tohoku and Kanto

TAKAGI, Rumi^{1*}, YOSHIOKA, Shoichi², MATSUMOTO, Takumi³

¹Dept. of Earth and Planetary Sci., Kobe Univ., ²RCUSS, Kobe Univ., ³Earthquake Research Department, NIED

1. Introduction

The Pacific plate is subducting beneath the Tohoku district, whereas the Philippine Sea plate is subducting beneath the Kanto district, overlapping on the top of the Pacific plate. In this study, firstly, we performed numerical simulations of temperature distribution associated with subduction of the Pacific plate beneath the Tohoku district. Secondly, based on the obtained temperature distribution beneath the Tohoku district, we performed numerical simulations of temperature distribution beneath the Kanto district, by incorporating subduction of the Philippine Sea plate.

2. Models and Methods

We calculated temperature distribution, using a 2-D box-type thermal convection model developed by Yoshioka and San-shadokoro (2002). We gave subduction velocity of the Pacific plate, referring to Sella et al. (2002). We changed the age of the subducting plate according to Sdrolias et al. (2006). Based on Nakajima et al. (2007, 2009) and Hirose et al. (2008), we gave the shape of the upper surface of the Pacific and the Philippine Sea plates. We used heat flow data of bore holes & heat probe (Tanaka et al., 2004; Yamano, 2004) and Hi-net in the wells (Matsumoto, 2007).

In the model of Takagi et al. (2011), mantle flow with high temperature took place near the tip of the mantle wedge associated with subduction of the Pacific plate beneath the Kanto district. This resulted in much higher calculated heat flow than observed one just above the tip of the mantle wedge with high temperature. Therefore, we constructed a domain where mantle flow does not flow into near the tip of the mantle wedge, which is referred to as the cold nose. Comparing observed heat flow data with those calculated from the temperature distribution obtained by numerical simulation beneath the Tohoku district, we constructed a temperature model which reproduces the observed heat flow values. We attempted to explain the observed low heat flow field spreading in the Kanto district, by subduction of the Philippine Sea plate in the model used for the Tohoku district.

3. Result

Incorporating the cold nose, we obtained a result which fits the observed heat flow values in the area of the oceanic side of the Tohoku district. In the Kanto district, the subduction of the Philippine Sea plate produced low heat flow region in the area of the landward side of the cold nose. To explain the observed heat flow values better in the Kanto district, we are also considering introducing frictional heating on the upper surface of the subducting Pacific plate.

Keywords: subduction, temperature distribution, flow field, heat flow, Kanto district, cold nose

Three-dimensional electromagnetic imaging of NE Japan

OGAWA, Yasuo^{1*}, ICHIKI, Masahiro², KANDA, Wataru¹

¹Volcanic Fluid Res. Centr., Tokyo Institute of Technology, ²Tohoku University

Geofluid plays an important role in the genesis of crustal earthquakes and volcanoes. Magnetotelluric method uses natural electromagnetic fields and it can image the fluid distribution in terms of electrical resistivity. We have selected an area around Naruko volcano for our project target in order to get detailed three-dimensional distribution of fluids in the crust with a horizontal resolution of ~3km. From the analyses of previous data of 60 MT stations, we have found (1)sub-vertical conductors at the active volcanoes, like Naruko and Onikobe and (2)lower crustal conductors with SSW-NNE strike in the backarc side, and (3)upper to middle crustal conductors in the forearc. We have found high seismicity, located over or outside the crustal conductors.

In this presentation, newly obtained 81 MT data over the two large calderas, Mukaimachi caldera and Sanzugawa caldera, and three-dimensional modeling results will be presented.

Keywords: geofluid, electromagnetic exploration, resistivity, earthquake, volcano, caldera

3D seismic velocity structure around Philippine Sea slab subducting beneath Kii Peninsula

SHIBUTANI, Takuo^{1*}, FUKUI, Taishi², HIRAHARA, Kazuro³, Setsuro Nakao¹

¹DPRI, Kyoto Univ, ²NIDEC, ³Science, Kyoto Univ

1. Introduction

Deep low frequency events (DLFEs) are distributed widely from western Shikoku to central Tokai (Obara, 2002; Kamaya and Katsumata, 2004; Obara and Hirose, 2006). Results from seismic tomographies and receiver function analyses revealed that the oceanic crust of the Philippine Sea plate has a low velocity and a high V_p/V_s ratio (Hirose et al., 2007; Ueno et al., 2008). Hot springs with high $^3\text{He}/^4\text{He}$ ratios are found in an area between central Kinki and Kii Peninsula despite in the forearc region (Sano and Wakita, 1985; Wakita and Sano, 1987). These phenomena suggest the process that H₂O subducting with the oceanic crust dehydrates at the depths of 30 - 40 km, causes the DLFEs, and uprises to shallower depths.

We carried out seismic observations in Kii Peninsula since 2004 in order to estimate the structure of the Philippine Sea plate and the surrounding area. We deployed seismometers along profile lines with an average spacing of ~ 5 km. We applied receiver function analyses and obtained images of S wave velocity discontinuities. In the previous presentation (Shibutani et al., 2010), we reported results for four profile lines in the NNW-SSE direction, that is the dip direction of the Philippine Sea plate and for a profile line in the NNW-SSE direction that is almost perpendicular to the dip direction. In this presentation we will report results of a seismic tomography in which we used information of seismic velocity discontinuities derived from the receiver function images and observed travel times at stations of the dense linear arrays.

2. Seismic travel time tomography

We implemented three dimensional geometry of the continental Moho, the upper surface of the oceanic crust and the oceanic Moho derived from the receiver function analyses to the velocity model. We used a fast marching method (de Kool et al., 2006) based on wavefront tracking for the theoretical travel time calculation. We also used observed travel times at temporary stations in the dense linear arrays in addition to permanent stations. A dense distribution of the temporary stations contributed to higher resolutions of tomographic images.

3. Structure around Philippine Sea slab

A result of the seismic tomography is shown in Fig.1. At the depth of 40 km the oceanic crust shows low velocity anomaly. As we go up to shallower depths, the low velocity anomaly seems to continue to the mantle wedge and to the lower crust. It becomes a large low velocity region at the depth of 16 km under the northwestern part of the Kii Peninsula. It is known that seismic activity is very high in the upper crust above the low velocity region. The low velocity anomaly is more significant in a western part of the Kii Peninsula.

We found differences also in the receiver function images between in the central to western part and in the eastern part. Beneath the former part, a low velocity region swells out into the mantle wedge from a dehydration area in the oceanic crust; the oceanic Moho becomes unclear below 40 km depth; the slab shows a convex upward bending shape. On the other hand, beneath the latter part, the oceanic Moho is uniformly clear down to 70 km depth; the slab shows a linear shape (Shibutani et al., 2010).

These features in the tomographic images and the receiver function images show that hydrous minerals in the oceanic crust are broken down by dehydration at the DLFE area, then the dehydrated fluids flow into the mantle wedge and the lower crust, and reduce the velocity in the regions. The differences in the structure and geometry of the slab and the mantle wedge between the central to western part and the eastern part of the peninsula can be explained by the amount of 'water' discharged into the mantle wedge and that left in the oceanic crust beneath 40 km depth through the dehydration.

We used waveform data from permanent stations of NIED; JMA; ERI, Univ. of Tokyo; Nagoya Univ. and DPRI, Kyoto Univ.

Keywords: tomography, receiver function, Philippine Sea slab, Kii Peninsula, slab-derived fluid

SCG65-P10

Room:Convention Hall

Time:May 20 17:15-18:30

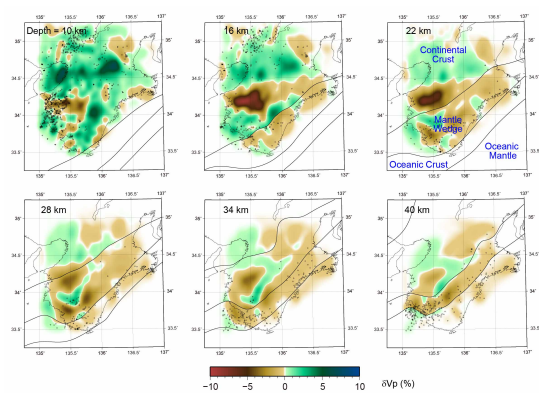


Figure 1 P wave velocity perturbation from an initial model at the depths of 10, 16, 22, 28, 34 and 40 km. The initial model is constructed basically on JMA2001 (Ueno et al., 2002) with a modification of -5 % velocity in the oceanic crust and +5 % velocity in the oceanic mantle and the mantle wedge. Circles indicate earthquakes which were used in the seismic tomography and occurred in the vicinity of each depth. The thick lines denote the continental Moho, the upper surface of the oceanic crust and the oceanic Moho from north to south.

Li/B RATIO OF CRUSH-LEACHED FLUID OBTAINED FROM THE SANBAGAWA METAMORPHIC BELT: ITS AREAL DISTRIBUTION

HIRAJIMA, Takao^{1*}, Yoshida Kenta¹, Sengen Yoshiteru¹, Noguchi Naoki¹, Kobayashi Tomoyuki², MISHIMA Taketoshi², Oh-sawa shinji²

¹Graduate School of Science, Kyoto University,, ²Institute for Geothermal Sciences, Graduate School of Sciences, Kyoto University

We investigated species and compositions of deep fluids trapped as fluid inclusions (FIs) in high-P met-amorphic rocks formed in the subduction zones. One of major goals of our deep fluid study is to testify an idea whether peculiar fluid soluble light elements, such as Li, B and Cl, can be used as an indicator of fluid generation depths in the subduction zones or not (Scambelluri et al. 2004).

Quantitative analyses of major and trace element composition of the deep fluid are still in the hard task. We adopted crush-leach (CL) technique (e.g., Banks and Yardley, 1992) for extracting FI from quartz veins/lenses developing parallel to the main foliation of Sanbagawa metamorphic rocks crystallized at 20 - 60 km depths.

Major cations/anions of CL fluids were analyzed by ion-chromatography, and Li and B were done by ICP-MS. Raman spectroscopy is adopted to determine the liquid and gas species of fluid inclusions in quartz. Microthermometry is adopted to estimate NaCl salinity and to identify the formation stage of FIs.

We extracted CL fluids from three areas of the Sanbagawa belt, 1) Wakayama area, 2) Asemigawa area and 3) Besshi area.

In Wakayama area, CL fluids were extracted from three samples of quartz veins hosted by metabasites covering the metamorphic grade from the chlorite zone, pumpellyite-actinolite facies equivalent, to the biotite zone, amphibolite facies equivalent. Their Li/B ratios increase with metamorphic grade of the host rocks from 0.02 to 0.10 (Sengen et al., 2009). The hydrochemical facies of CL fluids are X-HCO₃ type and the intermediate type between Na-Cl type and X-HCO₃ type. The texture of quartz grains, which retain FIs, show pervasively deformed and recrystallized type for all studied samples.

In Asemigawa area, CL fluids were extracted from six samples of quartz veins covering the metamorphic grade from the chlorite zone to the oligoclase-biotite zone. Their Li/B ratios mainly vary from 0.03 to 0.38, but there is no correlation between Li/B ratio and the metamorphic grade of host rocks. The hydrochemical facies of CL fluids are X-HCO₃ type, except for one sample of Na-Cl type. The texture of quartz grains show pervasively deformed and recrystallized type for all studied samples. Some host rocks show distinct S-C fabrics. These observations suggest the rocks in the Asemigawa area pervasively deformed during the exhumation stage.

In Besshi area, studied sample were collected from eclogite facies unit and neighboring schist units, equivalent with amphibolite facies. Li/B value of CL fluids varies from 0.10 to 1.99. Among all studied samples, relatively high Li/B (> 0.4 up to 2.0) ratio is identified only in this area. The samples with high Li/B ratio are characterized by both the Na-Cl type hydro-chemical facies and undeformed polygonal quartz fabric.

Two samples of quartz vein intercalated with eclogite show high Li/B ratio (0.27, 0.44), higher ratio of which is almost identical with those of dehydrated fluid from eclogite (Sengen et al., 2009; Marschall et al. 2007). Furthermore, CL fluids extracted from three samples of quartz veins intercalated with metasediments in the neighboring schist unit show much higher Li/B ratio (0.36-1.99). Yoshida et al. (2011) pointed out that Li/B ratio of dehydrated fluids was also controlled by the chemical composition of the host rock.

Raman spectroscopy and microthermometry clearly suggest that all samples applied CL technique contain fluids trapped at multi-stages, covering from prograde, peak and/or retrograde stages. However, some CL fluids obtained from quartz veins mostly free from post-peak deformation in the Besshi area have high Li/B ratio, which is almost identical with eclogite facies dehydrated fluids obtained from meta-serpentinite in Liguria and Betic Cordillera (Scambelluri et al. 2004). These facts suggest that Li/B ratio of dehydrated fluid has a potential for the indicator of the dehydration depth after considering some controlling factors.

Keywords: Deep fluid, Li, B, High-pressure metamorphic belt, Sanbagawa

Fluid infiltration and change in mass transfer during the exhumation of Sanbagawa metamorphic belt, Japan

UNO, Masaoki^{1*}, IWAMORI, Hikaru¹, NAKAMURA, Hitomi¹, ISHIKAWA, Tsuyoshi², Masaharu Tanimizu², YOKOYAMA, Tetsuya¹

¹Department of Earth and Planetary Sciences, Tokyo Institute of Technology, ²Kochi Institute for Core Sample Research, JAM-STE

Introduction: Individual parcel of regional metamorphic rock records physico-chemical conditions such as P-T path, mass transfer and deformation with the Lagrangian specification. On the other hand, a metamorphic belt as an ensemble of such parcels may provide a large-scale flow field of energy (e.g., temperature, entropy) and mass (including both solid and fluid phases with elements and isotopes) with the Eulerian specification. However, there are so far few models that integrate all the variables stated above. Phase petrology provides mostly the intensive variables (e.g., P-T path), whereas geochemistry provides mostly the extensive variables (time-integrated mass transfer), and these two have been treated separately. Here we combine phase petrology and geochemistry from a scale of mineral grain, and solve them under a simultaneous and consistent set of thermodynamic and mass balance equation. The results revealed the changes in mass transfer with changing P-T paths.

Method: The Sanbagawa metamorphic belt in Japan, the subduction-origin high-P type metamorphic belt, has been surveyed. To understand the nature of fluid during rehydration, we analyzed basic rocks that record retrograde reactions. Major and trace element compositions of each mineral, and bulk rock chemistry have been analyzed with EPMA, LA-ICP-MS, XRF and ICP-MS, respectively. Retrograde P-T path have been obtained by applying the Gibbs' method (e.g. Spear, 1993; Okamoto&Toriumi, 2001) to amphiboles and garnets.

Trace element budget along a specific P-T path were calculated by equating differential mass balance equation for major and trace elements as follows;

$$X_{fluid} dM_{fluid} = \text{Sum}(M_{solid} X_{solid}) + \text{Sum}(X_{solid} dM_{solid})$$

where X and M denote compositions and modes of minerals and dX and dM represent their changes along a specific P-T change. X_{solid} , M_{solid} , dM_{solid} for zoned minerals (amphibole and/or garnet) and X_{fluid} were derived from the results of Gibbs' method, X-ray map and fluid/mineral partition coefficients, respectively. Thus, the unknowns are dM s, and the equations are solved for them. As a result, the mass transfer during a specific P-T change ($X_{fluid} dM_{fluid}$) can be specified.

Furthermore, trace element budget during rehydration reactions were also constrained based on proportionality of bulk fluid-mobile element composition with H₂O (LOI (loss on ignition)). Based on a simple model that accounts for heterogeneity of protolith composition and devolatilization by dehydration reaction, the fluid composition during rehydration was estimated.

Results and Discussion: The P-T path obtained from the least rehydrated sample records the P-T path from 15kbar, 550°C to 11kbar 600°C, which corresponds to the exhumation just after the peak pressure condition. The mass balance analysis revealed that it was a dehydration reaction and Y and Cs increased whereas Ba decreased during this P-T path. No significant change was observed for Rb, Pb and Sr.

It is revealed that fluid mobile elements such as LIL elements, Sr and Pb are mostly proportional to LOI (loss on ignition). LOI and extent of rehydration are proportional in the Sanbagawa belt (Okamoto&Toriumi, 2005), thus the observed enrichment of LILE and Pb are interpreted to be associated with rehydration (from 11kbar 600°C to 3kbar 400°C). The Sr isotope ratios of the basic shists also increase with LOI, implying that the differences in bulk rock chemistry are due to an addition and/or reaction with external source of fluids with high ⁸⁷Sr/⁸⁶Sr. The estimated fluid composition is similar to calculated compositions of slab-derived fluids (Nakamura et al., 2008).

Comparing the results of (1) the mass balance analysis with early part of exhumation P-T path and (2) bulk composition analysis reveals that the mode of mass transfer changed from Y and Cs enrichment with Ba depletion, to LILE (Li, K, Rb, Cs, Sr, Ba) and Pb enrichment, associated with the change in P-T path.

Keywords: fluid, mass transfer, metamorphism, subduction zone, Sanbagawa metamorphic belt, trace element

Isotope and Boron of Quaternary lava in Central Sunda arc, Indonesia: an assessment of slab influence to mantle wedge

Haryo Edi Wibowo^{1*}, HASENAKA, Toshiaki¹, HANDINI, Esti¹, SHIBATA, Tomoyuki², Yasushi Mori³, HARIJOKO, Agung⁴

¹Department of Earth Science, Graduate School of Science and Technology, Kumamoto University, ²Beppu Geothermal Research Laboratory, Kyoto University, ³Kitakyushu Museum of Natural History and Human History, ⁴Department of Geological Engineering, Gadjah Mada University

We estimated contribution of slab-derived fluid of the arc mantle beneath Central Sunda Arc (CSA) in order to better understand the subduction processes. Sunda arc, a part of Pacific ring of fire, extends from Sumatera to Flores. Magmatism beneath Sunda arc is associated with subduction process. CSA is represented by a series of Quaternary volcanoes from fore arc toward back arc, consisting of Merapi, Merbabu, Telomoyo, Ungaran and Muria. We analyzed samples from these volcanoes by using X-Ray Fluorescence, Prompt Gamma-Ray and Instrumental Neutron Activation Analysis. Representative samples were also analyzed by Thermal Ionization Mass Spectrometer to obtain $^{87}\text{Sr}/^{86}\text{Sr}$ and $^{143}\text{Nd}/^{144}\text{Nd}$ ratios.

Boron is distinctively enriched in ocean floor sediment and altered oceanic crust (AOC). Higher mobility of boron from sediment to sediment-derived fluid than that of altered oceanic crust makes distinction of fluid sources. Fluid contribution to source mantle was estimated by applying ratio of boron and other mobile elements against HFSE. Estimation at CSA shows general decreasing trend of fluid contribution toward back arc with the highest contribution observed in the middle (Telomoyo) of arc transect, instead of the volcanic front (Merapi). This pattern is different from that estimated by Sr-Nd isotope ratios which are sensitive to modification of mantle by sediment-derived fluid. These isotope ratios show that influence of slab smoothly decreases from volcanic front toward back arc. Distinction between contributions from sediment-derived fluid and AOC-derived fluid was generated by plots of B/La, Rb/La, B/Nb, Rb/Nb against those of Sr and Nd isotope ratios. These plots show that the highest contributions of sediment occur at the volcanic front, whereas that from AOC occurs just a little behind the volcanic front. In addition to the variability of slab-derived fluid contribution, the small variation in isotopic and Nb/Zr, Nb/Ta ratios among fore arc volcanoes of CSA indicate little heterogeneity of the mantle source beneath them. Exception comes from the back arc volcano, Muria, which indicates relatively enriched mantle with only a little slab influence.

Keywords: Boron, Subduction, Slab fluid, Sunda arc

Development of A Preliminary Reference Rock Model for Physical Properties of Fluid-bearing Rocks

NAKAMURA, Michihiko^{1*}, WATANABE, Tohru², IWAMORI, Hikaru³

¹Department of Earth Science, Graduate School of Science, Tohoku University, ²Graduate School of Science and Engineering, University of Toyama, ³Department of Earth and Planetary Sciences, Tokyo Institute of Technology

Backgrounds: Recent advances in seismic tomography and magneto-telluric (MT) imaging have increased the potential for mapping the distribution of geological fluids (i.e., aqueous fluids and silicate melts) in the Earth's crust and uppermost mantle, since seismic velocity is sensitive to the fluid fraction, while electrical conductivity is strongly dependent on the connectivity of conductive fluid phases. To interpret the observed physical properties into the nature of the fluid, their correlation with the microstructure of fluid-bearing rocks is essential.

Sources of uncertainty: The seismic wave velocities are dependent on temperature and lithology, i.e., the phase and solid-solution compositions of the major minerals composing the rocks, besides on the fluid fraction. Especially in the middle and lower continental crusts, there is often considerable uncertainty regarding the lithology and temperature. Therefore, when the lithological and thermal structures are not well constrained, the uncertainties of the estimation of fluid distribution becomes large. On the other hand, the electrical conductivity is less dependent on the mineral compositions and phases, compared to the large contrast between those of silicate minerals and fluid phases. Although experimental data of electrical conductivity of minerals and fluids at elevated pressure and temperature are still insufficient, MT observations provide important constrains on the fluid distribution in the crust and mantle.

Scale resolutions of the geophysical imaging and length scale of geological heterogeneity: The observed seismic velocity is an average value typically in a km scale. Space resolution of the MT imaging is a few to tens of km, dependent on the depth. Given the high electrical conductivity in the middle to lower crusts of active convergent margins, interconnection of the fluid phases should be established in these km scales.

Role of heterogeneity: Since the dihedral angles between aqueous fluids and minerals in crustal conditions are generally larger than 60 degree, large fluid fraction is required for the fluid interconnection. The saline components in the fluids decrease the dihedral angle, but carbon dioxide increases, counteracting with each other. The veins and cracks can increase the fluid connectivity locally and anisotropically, but their individual length scale is much smaller than the imaging resolution. There are several other mechanisms to produce small scale heterogeneity or fabrics of the fluid distribution, but they may not responsible for the pervasive fluid interconnection in a km scale. Therefore, grain-scale fluid interconnection is still the first hypothesis to be tested. The relation between the volume fraction and connectivity of the pore fluids should be quantitatively understood for major crustal rocks.

The PROM project: In this context, we have reviewed and compiled the data of seismic velocities, electrical conductivities, and dihedral angles and other microstructural factors that determine the grain-scale fluid distribution for the rocks of crust and uppermost mantle. Although lack of the physical property data at elevated pressure and temperatures does not allow us to develop a comprehensive data base, a possible data set composed of some major rock types and their physical properties as a function of fluid fraction can be presented as a preliminary reference model for the crustal rocks.

Keywords: physical property of rocks, pore fluid, microstructure

Shear wave polarization anisotropy induced by C-type olivine LPO and fluid distribution beneath southern Kyushu

TERADA, Tadashi¹, HIRAMATSU, Yoshihiro^{1*}, MIZUKAMI, Tomoyuki¹

¹Department of Earth Sciences, Kanazawa University

A high V_p/V_s region detected by seismic tomography suggests the existence of fluid and serpentinized peridotite near the slab surface beneath the southern Kyushu region, Japan (Matsubara and Obara, 2011). The existence of fluid and serpentinite plays an important role for volcanism and seismicity in subduction zones. The distribution of fluid and serpentinite are, therefore, significant for considering the dynamics of subduction zones.

In this study, we perform the shear wave splitting analysis to detect the seismic anisotropy near the slab surface beneath the southern Kyushu region using shear wave splitting. In this study, we compare observations with theoretical values calculated from mineral elastic constants, discuss the cause of seismic anisotropy and infer the distribution of fluid and serpentinite beneath the southern Kyushu region.

We use events, whose source depth is greater than 30 km and magnitude is greater than 2.5, from 2004 to 2010 recorded at Hi-net stations in the southern Kyushu region. The observed polarization direction and delay time are NEE-SWW to NWW-SEE and 0.04-0.63 s, respectively. Previous works showed that the delay time is less than 0.3 s for shear wave splitting induced by the crustal anisotropy. The observed shear wave splitting whose time delay is greater than 0.3 s, therefore, originates from the seismic anisotropy in the mantle.

In the southern Kyushu region, a lot of split shear waves whose delay time is greater than 0.3 s pass through the high V_p/V_s region at the depth of 100-150 km. From the comparison of other ray paths, seismic anisotropy can be restricted in this region. The theoretical calculation shows that the Lattice Preferred Orientation (LPO) of C-type olivine fabric with the trench parallel b-axis and the trench normal c-axis inclined 60 degrees from the horizontal can reproduce the observations. We, therefore, suggest that C-type olivine fabric LPO causes the seismic anisotropy beneath the southern Kyushu and the thickness of the anisotropic layer is estimated to be about 13-30 km. This result suggests also that the existence of fluid in this region. We, thus, consider that the migration of interstitial fluid in peridotite is activated due to a decrease of the dihedral angle of olivine fluid interface (Mibe et al., 1999) at the depth below 100 km beneath the southern Kyushu region.

In this study, we observe no shear wave splitting induced by serpentine in the forearc mantle wedge. This result does not contradict the existence of a thin serpentine layer (1~3 km) proposed by Hilairet and Reynard (2009).

Keywords: shear wave polarization anisotropy, C-type olivine, LPO, fluid, serpentine

SYNTHETIC EXPERIMENTS OF AQUEOUS AND CARBONATE FLUID INCLUSIONS

OHI, Shugo^{1*}, Tetsu Kogiso¹, Takao Hirajima²

¹Human and Environmental studies, Kyoto University, ²Science, Kyoto University

Deep aqueous fluids from subducted slab affect volcanic activity and seismicity in the subduction zone. (e.g., Schmidt and Poli, 1998) To reveal the chemistry of slab-derived fluids is crucial for understanding the material circulation in subduction zones, but as yet it is very difficult to experimentally constrain the chemical composition of these fluids. Diamond-trap experiments in combination with LA-ICP-MS analyses of frozen samples have been used to analyze chemical compositions of aqueous fluids in equilibrium with complex mineral assemblages (e.g., Kessel et al., 2004). However, in order to accurately determine fluid compositions experiments also need to be designed to account for modification of the fluid during quenching. Synthetic fluid inclusions trapped during high-pressure experiments can keep the composition of the fluids produced at run conditions. We have developed a method to trap fluids liberated during decomposition of hydrous and carbonate minerals as fluid inclusions in a quartz crystal.

The synthetic fluid inclusion technique (Sterner and Bodnar, 1984) was employed in this study. Synthetic fluid inclusions were formed in synthetic quartz provided by Nihon Dempa Kogyo Co., LTD. Quartz single crystals were cut into about 1-2mm size, heated to 450 C, and then quenched in cold distilled water to make cracks within it. After drying in a vacuum oven at 150 C overnight, the quartz crystals with cracks were rapped in a piece of Pt foil (2.5um-thick) and sealed in Au or Pt capsules with various mineral assemblages, such as Mg(OH)₂, CaCO₃+SiO₂, CaCO₃+SiO₂+H₂O and mMgCO₃Mg(OH)₂nH₂O+SiO₂+Mg(OH)₂. The capsule was placed in a solid-media piston-cylinder apparatus and kept at the pressure range 0.5-1 GPa and at the temperature range 800-1100 C for 3-192 hours.

After quenching, thin sections (200-500um-thick) were prepared to examine with an optical microscope, Raman spectroscopy and microthermometry. The analyses for microthermometry were performed by referring Diamond (2001) and using the computer program Loner AP (e.g., Bakker, 2009).

Fluids liberated from Mg(OH)₂ were successfully trapped as fluid inclusions in all experiments. Microthermometry for a fluid inclusion in the sample synthesized at 800 C and 1 GPa for 3 hours showed the homogenization temperature of 251 C, molar volume of 22.8 cm³/mol. However, the calculated isochore shows that the temperature calculated for 1 GPa was 961 C, which was different from the run condition.

Fluid inclusions were not observed in experiments with CaCO₃+SiO₂, whereas were successfully synthesized in experiments with CaCO₃+SiO₂+H₂O. The size and amount of fluid inclusions in these samples were smaller than those in the experiments with Mg(OH)₂. Raman spectra showed the peaks of CO₂ but the broad peaks of H₂O were not observed clearly.

Fluids liberated from mMgCO₃Mg(OH)₂nH₂O+SiO₂+ Mg(OH)₂ were successfully trapped as fluid inclusions in all experiments. Raman spectra showed that the fluid inclusions in these samples were composed of H₂O and CO₂. Microthermometry for the three fluid inclusions in the sample synthesized at 850 C and 1GPa for 18 hours showed that the homogenization temperatures from vapor-liquid carbon phase to liquid carbon phase were 24-29.5 C and total homogenization temperatures were 255-269 C, yielding molar volumes of 24.2-26.3 cm³/mol and total mole fractions CO₂ of 12-18 mol%. The calculated isochores give 910-1033 C at 1GPa, which had wide distribution.

In the experiments of anhydrous systems, liberated fluid could not be trapped during crack healing or perhaps crack healing did not occur in the experimental conditions in present study. The temperatures estimated from microthermometry were different from run conditions.

To interpret the condition that fluid inclusions are produced, it is needed to figure out the reason of this discrepancy by more analyses with precise observations of occurrence.

Keywords: synthetic fluid inclusion, hydrous mineral, carbonate mineral, piston-cylinder

Measurement of seismic velocity of crustal rocks under high confining pressure and pore pressure

HARADA, Yuya^{1*}, KATAYAMA, Ikuo²

¹Department of Earth and Planetary Systems Science, Hiroshima University, ²Department of Earth and Planetary Systems Science, Hiroshima University

Introduction

Water of the earth interior is mainly supplied at the subduction zone and has important role on seismic activity and volcanism in island arc. It is guessed that slow slip events and tremors occurring at this region are related to water. Based on the seismic tomography at Kanto district, high Poisson's ratio area (~ 0.337) was observed and suggested weak seismic coupling (Kamiya and Kobayashi., 2000). Similar high Poisson's ratio is detected at Tonankai and Sikoku district, exceeding 0.3. Those regions correspond to the plate boundary generating slow slip events or tremors (Kodaira et al., 2004 ; Shelly et al., 2006). Because relatively young oceanic plates are subducting in districts from Kanto to Shikoku, antigorite which Poisson's ratio is ~ 0.29 may exist stably in those areas. In this case, the observed high Poisson's ratio requires excess pore fluids in addition to the serpentinized mantle. In order to clarify geometry and the abundance of water, we investigate seismic velocity of crustal rocks under high confining pressure and pore fluid pressure.

Experimental methods

For the measurement of seismic velocity, we used the hydraulic pressure vessel in Hiroshima University, in which seismic wave velocity was calculated by using pulse echo method. Samples are gabbro (from Belfast) and granite (from Inada) and were prepared into a cylindrical shape, which diameter and length is 20 and 5-10 mm. We measured seismic velocity under dry and wet conditions, in the later case, distilled water is supplied into the sample with pore pressure up to 50 MPa.

Results and discussion

Under dry experiments, seismic velocities of gabbro and granite were measured up to confining pressure as high as 200MPa. Calculated seismic velocities of gabbro in each confining pressure (100, 140, and 180MPa) were $V_p = 6.88, 6.94, 6.83$ km/s, $V_s = 3.85, 3.91, 3.79$ km/s, and velocities of granite were ranging $V_p = 4.94-6.09$ km/s and $V_s = 2.89-3.36$ km/s under confining pressure of 200 MPa. These values are lower than Christensen (1996)'s experiments, but V_s of gabbro are similar to those values. From the measurement of both compression and decompression process, it is confirmed that velocity variation has the reproducibility and there is an effect depending on cracks or pores closed by high confining pressure.

Under wet experiments, granite was measured at confining pressure of 60 MPa with pore pressure of 50 MPa (effecting pressure of 10 MPa). At confining pressure of 60 MPa before raising pore pressure, velocities were $V_p = 5.17-5.60$ km/s and $V_s = 2.84-4.36$ km/s. After pore pressure increased to 50MPa, velocities were slightly changed to $V_p = 5.02-5.18$ km/s, $V_s = 2.13-3.64$ km/s. However, signal from the sample reflection is very weak and therefore these values have large uncertainty at this moment. It is likely that this pulse weakening is related to the wave splitting, overlapping with background noises, and the reflectivity between the sample and the spacer of sample assembly. We try to fix these issues and hope to present the effect of pore pressure on seismic velocity in the coming JPGU meeting.

Keywords: seismic velocity, crustal rock, Poisson's ratio, geofluid, pore pressure, subduction zone

A three-dimensional electrical conductivity distribution model of the upper mantle beneath Tohoku district

ICHIKI, Masahiro^{1*}, OGAWA, Yasuo², Songkhun Boonchaisuk², DEMACHI, Tomotsugu¹, FUKINO, Hiromi⁴, HIRAHARA, Satoshi¹, HONKURA, Yoshimori², KAIDA, Toshiki¹, KANDA, Wataru², KONO, Toshio¹, KOYAMA, Takao³, MATSUSHIMA, Masaki⁴, NAKAYAMA, Takashi¹, SUZUKI, Syuichi¹, TOH, Hiroaki⁵, UYESHIMA, Makoto³

¹Grad. Sch. of Sci., Tohoku Univ., ²Volcanic Fluid Res. Center, Tokyo Tech, ³Earthq. Res. Inst., Univ. Tokyo, ⁴Grad. Sch. of Sci. and Eng., Tokyo Tech, ⁵Grad. Sch. of Sci., Kyoto Univ.

While plenty of three-dimensional (3-D) seismic tomographic images has been revealed (e.g. Zhao et al., 1992; Nakajima et al., 2001), only a few 3-D electrical conductivity distribution model has been proposed in terms of wedge mantle in subduction zones (e.g. Patro et al., 2007). Introducing the state-of-the-art mobile magnetotelluric (MT) observation systems (LEMI-417 and NIMS), we have acquired MT data at Tohoku district, northeastern Japan for the aim of 3-D electrical conductivity distribution in the wedge mantle. Typical observation duration are three months at each site, and MT response functions from 10 to 20000 seconds in period have successfully collected with fine quality. The site location is arranged with ca. 20 km interval. The MT phase response functions at many sites show over 90 degrees over 5000 seconds and suggest that 3-D distribution beneath this area.

Simple checker board resolution tests have been performed to estimate resolution. Regular cubes with 40 km on side and 10 ohm-m in conductivity embedded in 1000 ohm-m matrix were clearly recovered down to 120 km in depth using the synthetic data, while those with 20 km on side were not recovered clearly.

We carried out the three-dimensional inversion analysis with WSINV3DMT code (Siripuvaporn et al., 2005). Although the inversion process is still on the way and the conversion is not enough, the east-west profile (across the Japan Arc) of the preliminary result shows that conductive region appears at about 120 km in depth beneath back-arc region and elongates obliquely towards the volcanic front. The north-south profile (along the Japan Arc) shows the vertical conductive and resistive columns appears alternatively. That basic images are well consisted with the seismic tomographic model (Nakajima et al., 2001), provided that conductive and low velocity zone should corresponds with each other. Obtained the final 3-D model, our final destination is to estimate the mantle geotherm and fluid distributions in the wedge mantle using seismic tomographic and electrical conductivity images.

Numerical analyses of water content and melting regimes in the NE Japan arc

HORIUCHI, Shyunsuke^{1*}, Iwamori Hikaru²

¹Earthquake Research Institute, The University of Tokyo, ²Tokyo Institute of Technology

Melting and seismic structure beneath the northeast Japan arc considering upon the uncertainties of H₂O content is modeled to estimate the relation between melting region and H₂O content, and restrict water content distributed in mantle wedge. This model results show that increasing water content, a weak melting starts to occur beyond $C_{H_2O} = 0.07$ wt%, and the calculated P-wave and S-wave velocity structures between $C_{H_2O} = 0.10$ wt% and 0.40 wt% can explain tomographic low velocity zones. The distribution of melt production rate ($C_{H_2O} = 0.15$ wt%) shows that all three mechanism (Flux, decompression, and compression melting) are necessary to explain volcanic activity at back arc, volcanic front, and intermediate region in the Northeast Japan arc. In the case of $C_{H_2O} = 0.15$ -0.34 wt%, the model results of volcanic eruption rate can explain observed across-arc features in terms of relative intensities (i.e., spatial location and pattern). Considering into the comparison with tomographic data, melting mechanism, and the comparison with volcanic eruption data, this model results for $C_{H_2O} = 0.15$ -0.34 wt% can explain volcanic activity in the Northeast Japan arc.

Keywords: water, melting, subduction zone